Journal of Energy Storage 178 (2026) 123578

Contents lists available at ScienceDirect

Journal of Energy Storage

journal homepage: www.elsevier.com/locate/est

Research Papers

Market-based optimization of the energy-to-power ratio of a latent thermal energy storage unit-based Carnot Battery

Lauritz Zendel [a,*], Jonathan Stelzer [b], Frank Dammel [a], Wolf Fichtner [b], Peter Stephan [a]

[a] Technical University of Darmstadt, Department of Mechanical Engineering, Institute for Technical Thermodynamics, Peter-Grünberg-Straße 10, Darmstadt, 64287, Hessen, Germany

[b] Karlsruhe Institute of Technology (KIT), Department of Economics and Management, Institute for Industrial Production, Chair of Energy Economics, Hertzstraße 16, Karlsruhe, 76187, Baden-Württemberg, Germany

ARTICLE INFO

Keywords:
Pumped thermal electricity storage
Carnot battery
Day-ahead market
Phase change material
Energy-to-power ratio

ABSTRACT

The volatile electricity generation from renewable energies creates the need for electricity storage technologies which, unlike the pumped hydroelectric energy storage established to date, are not tied to geographical conditions. The emerging technology of pumped thermal electricity storage (PTES) is one such alternative. PTESs belong to the group of Carnot Batteries.

Using a price-taker approach with perfect daily foresight, this study determines the achievable contribution margin of a 5 MW generic storage in the German day-ahead market by exclusively exploiting daily price spreads. Based on real data from various phase change materials, the investment costs for PTES with a latent thermal energy storage (LTES) unit can be determined as a function of their energy-to-power ratio (E/P-ratio). By comparing the achievable contribution margins and investment costs, the most economical E/P-ratio can be identified. The result is a cost-optimal E/P-ratio that depends on the year, the round-trip efficiency (electricity to electricity), the coefficient of performance, and the power-related purchased equipment cost. For this purpose, both historical and future years were examined, whereby an agent-based market model was used to simulate the future electricity price time series. Oxalic acid dihydrate proved to be a promising phase change material for all round-trip efficiencies investigated. It turned out that, under the assumed boundary conditions, no PTES enables an economically attractive operation at round-trip efficiencies between 30 % and 70 %. The configurations closest to an economically attractive operation have E/P-ratios of at least 4 h related to the charging duration at half discharging duration.

1. Introduction

In order to limit global warming to less than 2 °C or even 1.5 °C, decisive action to reduce greenhouse gas emissions across all sectors is essential in the coming years [1]. One measure to reduce greenhouse gas emissions is the expansion of renewable energies, which is already having a positive impact on the emission curve, with wind and photovoltaic (PV) having a major influence [2]. This is also reflected in the exponential increase in global electricity generation from wind [3,4] and PV [4,5] in recent years. Nevertheless, a tripling of installed wind and PV capacity by 2030 compared to 2022 would be necessary to achieve the goals of the Paris Agreement [6]. The increasing share of renewable energies requires more flexibility in the operation of the energy system [6], whereby energy storage technologies can support the integration of renewable energies [7,8]. While PHES still account for more than 90 % of total global electricity storage capacity in 2020, grid-scale battery storage such as lithium-ion batteries are catching up [8]. Another emerging energy storage technology is the Carnot Battery (CB), which has met with increasing interest, especially in recent years [9]. In contrast to PHES, CBs do not suffer from geographical constraints [9–11] and large space requirements for installation [11].

A subgroup of CBs is the PTES [9,10]. A PTES stores electricity by converting it to heat [11]. One possibility for further subdivision is the distinction between Brayton and Rankine cycles for the charging (heat pump (HP)) and discharging (heat engine (HE)) process [9,10]. In addition, the HP can be extended [11] or replaced [12] by an electric heater for the charging process. While Brayton PTES are most frequently coupled with sensible thermal energy storage units, Rankine PTES are suitable for operation with LTES units [10]. Nevertheless, opposite or combined couplings can also be found in the literature. For example, Rankine PTES are experimentally coupled to sensible thermal

* Corresponding author.
E-mail address: zendel@ttd.tu-darmstadt.de (L. Zendel).

https://doi.org/10.1016/j.est.2026.123578
Received 28 July 2025; Received in revised form 30 June 2026; Accepted 6 July 2026
Available online 15 July 2026

Nomenclature

Abbreviations

AA	Adipic acid
AC	Ammonium chloride
ADO	Adonitol
BHO	Barium hydroxide octahydrate
BW03	Beeswax with 0.3 % graphene
CAPEX	Capital expenditure
CB	Carnot Battery
CEPCI	Chemical Engineering Plant Cost Index
CM	Contribution margin
COP	Coefficient of performance
ERY	Erythritol
E/P-ratio	Energy-to-power ratio
HDPE	High-density polyethylene
HE	Heat engine
HP	Heat pump
LAES	Liquid air energy storage
LCOS	Levelized cost of storage
LTES	Latent thermal energy storage
MAN	Mannitol
MCH	Magnesium chloride hexahydrate
MNH	Magnesium nitrate hexahydrate
MNHLN	Magnesium nitrate hexahydrate with lithium nitrate
OAD	Oxalic acid dihydrate
OPEX	Operational expenditure
PCM	Phase change material
PEC	Purchased equipment cost
PFSF	Potassium formate with sodium formate
PHES	Pumped hydroelectric energy storage
PNSN	Potassium nitrate with sodium nitrite
PTES	Pumped thermal electricity storage
PV	Photovoltaic
SA	Sebacic acid
SC	Sodium chloride
SN	Sodium nitrate
SNPN	Sodium nitrate with potassium nitrite
SoC	State of charge
SoC_0	Initial state of charge
WACC	Weighted average cost of capital

Symbols

A	Capacity parameter, m^3
C	Heat capacity, kJ
$CAPEX$	Capital expenditure, €
COP	Coefficient of performance, -
E/P-ratio	Energy-to-power ratio, h
$Expenses(t)$	Expenses at hour t, €
EXR	Exchange rate, € $^{-1}
f	Factor, -
h	Specific enthalpy, $kJ\,kg^{-1}$
i	Interest rate, %
l	Length, m
$LCOS$	Levelized cost of storage, €cent kWh^{-1}
m	Mass, kg
n	Quantity, -
$OPEX$	Operational expenditure, €
p	Price, € kWh^{-1} / € kg^{-1} / € m^{-1}
P	Power, W
PEC	Purchased equipment cost, $
r	Radius, m
R	Ratio, -
$Revenue(t)$	Revenue at hour t, €
$s(t)$	Operating duration at hour t, h
SoC	State of charge, h
t	Time, h
T	Temperature, °C / K
V	Volume, m^3

Greek symbols

η	Efficiency, -
ρ	Density, $kg\,m^{-3}$

Subscripts and superscripts

0	Initial (beginning of the day)
char	Charge
dis	Discharge
E	End of system lifetime
el	Electricity
ex	Exergetic
grid	Electricity grid
HTF	Heat transfer fluid
i	Inner/mathematical index
lit	Literature
n	Year
o	Outer
P	Power
PC	Phase change
rt	Round-trip
s	Solid
study	Present study
tot	Total
USD	US Dollar

energy storage units [13], and Brayton PTES are extended by latent energy storage [14] or considered in combination with LTES [15].

For each possible configuration of a PTES, the question arises as to the dimensioning of the individual components, with the thermal energy storage being of particular importance as it defines the storage capacity of the PTES. Both the energy market in which a PTES is integrated and the selected thermal energy storage must be taken into account in this process. This will be discussed in the following.

1.1. Electrical energy storage systems in energy markets

Individual PTES configurations can vary in terms of the capacity of the storage unit in relation to the electrical power. This variable is referred to as E/P-ratio [16,17] and in the context of this work, the E/P-ratio is defined as the duration that the heat pump cycle can run at maximum power until the storage unit is considered to be fully charged. There are also other definitions of the E/P-ratio in the literature, for example as the ratio of storage capacity to discharge power [18,19]. In those cases where the discharge power is recognizably used for the definition of the E/P-ratio, it is explicitly highlighted as E/P-ratio$_{dis}$.

The influence of the E/P-ratio on the economic performance of electrical energy storage systems has already been the subject of studies. A comprehensive study of the potential contribution margin (CM) from price spreads in several day-ahead markets was conducted by Mercier et al. [18]. The study examined the EU-28 countries as well as Norway, Switzerland and Turkey for the period from 2000 to 2021. The authors determined a maximum E/P-ratios$_{dis}$ of 4 h to 6 h hours, which, if exceeded, does not lead to a significant increase in the CM in any of the countries investigated. Major country-specific differences were identified. In addition, the achievable CM varies over the years. Two important findings, namely the importance of regional and temporal dependency, were also found by Connolly et al. [20] for a PHES with a given E/P-ratio.

In addition to cross-national studies [16,18], there are also country-specific studies. Various European countries [21–24], including Germany [17,25–27], were investigated.

1.2. Dimensioning of LTES units

One form of thermal energy storage is represented by LTES. A PCM that experiences a phase change and thereby absorbs or releases energy is used in an LTES unit [28]. Particularly relevant here are PCMs that undergo a phase change from solid to liquid and vice versa [28]. Since PCMs have a low thermal conductivity, measures to enhance heat transfer such as fins and nanoparticles, are being considered [29,30]. This, however, makes the design and dimensioning of an LTES unit more complex.

When dimensioning LTES units, the boundary conditions resulting from the system into which they are integrated must be taken into account [31]. This includes the required heat capacity and heat flow [31]. Given a specific geometry, the driving temperature difference in an LTES unit can be adjusted to achieve the required heat flow [32] whereby a variable temperature difference can also be used [33]. A systematic variation of geometry parameters [34], e.g., with the aim of minimizing the storage volume [35], can also be part of the design process. However, the choice of geometry, e.g., the number of tubes used in an LTES unit, has an impact on costs [35]. An accurate cost estimate requires knowledge of the materials used and a detailed breakdown of the geometry.

1.3. Dimensioning of CBs in energy systems

Several attempts have been made to link the macro perspective of energy systems and markets with the system-level design of CBs. In addition to PTES, which have already been introduced, liquid air energy storage (LAES) also belong to the group of CBs [10,19]. LAES store energy by liquefying air and storing it at cryogenic temperatures [10,19,36].

The potential of an LAES that benefits from price fluctuations in the UK real-time electricity market to achieve a CM was investigated by Lin et al. [37]. The three main components of the LAES, consisting of the liquefaction unit, storage tank and discharge unit, are dimensioned using a genetic algorithm in order to optimize the net present value.

The economic performance of an LAES on the UK electricity market is examined by Vecchi et al. [19]. CMs from price spreads and reserve markets were taken into account. An E/P-ratio$_{dis}$ of 2-3 h was identified as an optimum when all markets were considered. If only price spreads were allowed to generate a CM, an E/P-ratio$_{dis}$ of 4-5 h was found to be optimal.

An optimal size of a PTES was determined by Tassenoy et al. [38]. For this purpose, the investment costs per MW of the HP and the HE as well as the investment costs per MWh of the sensible thermal energy storage were considered. Although it turned out that none of the configurations justifies the investment in a PTES from an economic point of view, the methodology presented enables cost-optimized dimensioning of the thermal energy storage.

Dumont et al. [39] propose a methodology for dimensioning a PTES that aims at peak shaving. The tank of the thermal energy storage was dimensioned in such a way that the daily heat demand peaks could be covered. The case study revealed a payback period for the PTES of slightly more than six years.

1.4. Scope of the present study

As the literature review shows, there is a lack of studies that take a holistic perspective in the design of LTES based PTES. The present study aims to address this gap.

A detailed examination of an LTES unit is carried out in order to answer the following research question:

1. Which PCMs enable the lowest possible costs in an LTES unit based PTES?

The following question arises with regard to the dimensioning of the LTES unit in the PTES, which is reflected by the E/P-ratio:

2. Which E/P-ratios allow for the most economical operation of the LTES unit based PTES?

As the results of [18] clearly demonstrate, it is advisable to focus on one market area and a limited time period. The following third research question should therefore be answered:

3. Would it have been economically attractive to operate an LTES unit based PTES with an electrical input power of 5 MW on the German electricity market in 2023 and 2024, and is economically attractive operation realistic in the future?

This requires various assumptions to be made when creating the underlying future scenarios, which leads to the fourth and final research question:

4. Under which conditions would it be economically attractive to operate an LTES based PTES in the future?

Further assumptions that specify the research questions of this study are explained in the subsequent chapter, along with the rationale behind them. The following important limitation of the study applies: Even though some studies show that the reserve markets have considerable economic potential [17,27], these markets are not included in the present study. This is based on the expectation that the market volume for automatic Frequency Restoration Reserve and manual Frequency Restoration Reserves will not be sufficiently large in the future to be a representative case for large-scale applications of PTESs. This assumption is supported by current data from the Federal Network Agency [40]. These markets are expected to be served by other technologies, which limits the potential for new technologies to achieve profitability.

2. Material and methods

This chapter describes the methodology on which the present study is based and the material required for its application. The PTES examined in this study consists of a HP, an LTES unit, and a HE. No cold storage is involved. Due to the abstract consideration of HP and HE presented below, this study is not limited to a specific PTES design.

2.1. Influencing parameters investigated

The aim of this study is to determine the optimal E/P-ratios and the associated PCMs based on market prices. For this purpose, both the achievable CM and the associated investment costs of each configuration must be determined. To this end, the influencing parameters that will be examined in more detail in the further course of this study are presented and categorized. These are as follows:

1. Electricity price time series
2. Round-trip efficiency (η_{rt})
3. Energy-to-power ratio (E/P-ratio)
4. Coefficient of performance (COP)

Table 1
Influencing parameters, parameter ranges and parameter step sizes.

Influencing parameter	Parameter range	Parameter step size
Electricity price time series	2023, 2024, 2030, 2035	–
η_{rt}	30–70 %	5 %
$E/P\text{-}ratio$	1–10 h	1 h
COP	2.25–3.50	0.25
$PEC_{HP,HE}$	1–6 M$	1 M$
$R_{char,dis}$	2	–
SoC_0	0–10 h	1 h

5. Power-related purchased equipment cost ($PEC_{HP,HE}$)
6. Ratio between charging and discharging duration ($R_{char,dis}$)
7. Initial state of charge (SoC_0)

The CM is influenced by the parameters electricity price time series (1), round-trip efficiency (2), E/P-ratio (3), ratio between charging and discharging duration (6), and initial state of charge (7). Round-trip efficiency (2), E/P-ratio (3), COP (4), and the power-related PEC (5) have an influence on the investment costs in the context of this study. The following explains how the parameters mentioned affect the CM and the power-related PEC. The electricity price time series depends on the year under consideration and directly influences the CM through the course of the electricity price. Higher round-trip efficiencies ensure higher profits per charge and discharge cycle and also allow more hours to be used profitably. An increase in E/P-ratio enables an extension of usable hours. The rise in the latter two parameters therefore leads to an increase in the CM. An upward trend in the ratio between charging and discharging duration leads to an increase in discharge power and price peaks being better exploited, which is why an increase also has a positive effect on the achievable CM. As far as the SoC_0 of the storage unit is concerned, it is not possible to determine a generally valid influence on the achievable CM without taking into account the specific electricity price time series. However, the ratio between charging and discharging duration and the SoC_0 are defined based on the explanations in Sections 3.2 and 3.3 and are therefore not variable for the final analyses.

A change in the round-trip efficiency has an effect on the efficiency of the subsystems and therefore also on the exergetic efficiency, i.e., the quality grade of the HP. For a prescribed COP, a change in the exergetic efficiency of the HP results in a varying temperature level. This means that the available PCMs characterized by their phase change temperature also change. Consequently, the round-trip efficiency has an impact on the capacity-dependent PEC. It should be emphasized at this point that the specification of the COP and the round-trip efficiency is hypothetical, so that implementation in a real system is not necessarily feasible. Temperature differences during heat transfer and isentropic efficiencies of less than one in compression and expansion machines are typical reasons why it is difficult to achieve high efficiencies in real systems. Both an increase in the E/P-ratio and the COP increase the required capacity of the LTES unit and thus also the capacity-dependent PEC. While a higher E/P-ratio requires longer charging and therefore larger storage capacity, an increased COP results in more thermal energy that must be stored per unit of electrical energy used, thus having the same effect. These capacity-dependent PEC and the power-related PEC make up the total PEC. The range of the influencing parameters and, if applicable, the step size of these parameters are listed in Table 1. $R_{char,dis}$ is specified as 2. In exceptional cases prior to Section 3.4, a value of 1 is used instead, corresponding to an equal charging and discharging duration, which is indicated in each case.

The optimization is influenced by the CM effecting parameters and is described in the following section. The origin of the electricity price time series for this optimization is explained in the two subsequent Sections 2.3 and 2.4. The PEC calculation of the LTES unit and the selection of the PCMs are then presented in Sections 2.5 and 2.6, so that the economic viability of the PTES can be assessed using the quantities described in the last two sections.

2.2. Optimization problem

In order to evaluate the CM of a PTES on the German electricity market, an optimization model was developed using the Python-based modeling language Pyomo [41,42]. The solver GLPK was used to provide a solution to the problem.

A generic electrical energy storage model was developed for the optimization. The properties of the PTES are only explicitly taken into account when calculating the PEC of the LTES unit. Market power is neglected, so that the assumption of a price-taker applies. A perfect daily price forecast with hourly resolution is assumed and the optimization takes place on a daily basis.

The objective function is given as follows:

$$\max\left(\sum_{t=0}^{23}\left(Revenue(t) - Expenses(t)\right)\right) \tag{1}$$

which corresponds to the CM, excluding other variable operating costs apart from the purchase of electricity, with

$$Revenue(t) = P_{char} \cdot f_P \cdot \eta_{rt} \cdot p_{el}(t) \cdot s_{dis}(t) \tag{2}$$

$$Expenses(t) = P_{char} \cdot (p_{el}(t) + p_{grid}(t)) \cdot s_{char}(t) \tag{3}$$

where P_{char} is the electrical charge power. The discharge power takes twice the value of P_{char} in the case of halved discharging duration, which is described by f_P:

$$f_P = \begin{cases} 1 & \text{Equal charging and discharging duration} \\ 2 & \text{Halved discharging duration} \end{cases} \tag{4}$$

The round-trip efficiency is denoted by η_{rt}. The electricity price of the respective hour $p_{el}(t)$ is taken into account for the discharge process, while an additional grid fee of 12.01 €MWh^{-1} is added for the charge process, as for a battery electrical energy storage located in Aachen (Germany) [17]. $s_{dis}(t)$ and $s_{char}(t)$ are the operating durations for the discharging and charging process at hour t. These operating durations can have the integer values 0 h and 1 h and in the case of a halved discharging duration, $s_{dis}(t)$ can additionally take the value 0.5 h. Consequently, the operating durations represent the variables of the optimization problem.

The following constraints apply to the optimization. In each hour, the state of charge (SoC) of the PTES must not fall below 0 h taking into account the offset due to SoC_0:

$$\sum_{t=0}^{t_i}\left(s_{char}(t) - f_P \cdot s_{dis}(t)\right) + SoC_0 \geq 0\,\text{h} \quad \forall t_i \in [0,23] \cap \mathbb{Z} \tag{5}$$

In addition, the E/P-ratio, also including SoC_0, must not be exceeded at any time:

$$\sum_{t=0}^{t_i}\left(s_{char}(t) - f_P \cdot s_{dis}(t)\right) + SoC_0 \leq E/P\text{-}ratio \quad \forall t_i \in [0,23] \cap \mathbb{Z} \tag{6}$$

The SoC_0 is given in hours. An empty storage corresponds to the SoC_0 of 0 h, whereas a value of the SoC_0 equal to the E/P-ratio represents a fully charged storage.

At the end of the day, the SoC must be the same as at the beginning:

$$\sum_{t=0}^{23}\left(s_{char}(t) - f_P \cdot s_{dis}(t)\right) = 0\,\text{h} \tag{7}$$

Finally, charging and discharging are prevented from taking place simultaneously:

$$s_{\text{char}}(t_{\text{i}}) + s_{\text{dis}}(t_{\text{i}}) \leq 1\,\text{h} \quad \forall t_{\text{i}} \in [0, 23] \cap \mathbb{Z} \tag{8}$$

2.3. Day-ahead market data

The input data for the historical electricity market prices for 2023 and 2024 originate from the Federal Network Agency [43]. An hourly resolution of the prices was chosen. Logarithmic histograms of the price distribution for the two years can be seen in Fig. A.1. The average electricity price in 2023 is $95.18\,€\,\text{MWh}^{-1}$, and $78.55\,€\,\text{MWh}^{-1}$ in 2024. The standard deviation is higher in 2024 with a value of $52.79\,€\,\text{MWh}^{-1}$ than in 2023, where it has a value of $47.57\,€\,\text{MWh}^{-1}$. The quotient of standard deviation and mean value, which is referred to as relative standard deviation in Wilson et al. [25], is therefore higher in 2024. According to the results of Wilson et al. [25], this leads to the expectation of a higher achievable CM for PTESs in 2024. The relative standard deviations for the historical data are 49.98 % in 2023 and 67.20 % in 2024.

2.4. Future market data

This study also examines the economics of the storage system under potential market price scenarios for the years 2030 and 2035 to reflect possible future market conditions. To this end, a scenario is simulated using the agent-based electricity market model PowerACE [44], from which corresponding market prices are derived. PowerACE simulates the day-ahead electricity market with hourly resolution up to the year 2050, covering multiple market regions. The model includes the hourly dispatch planning and operational simulation of power plants, taking into account factors such as electricity demand, renewable energy generation, resource availability, and technical constraints. In this framework, renewable generation and demand profiles are treated as exogenous inputs, whereas conventional generation units and storage systems are modeled as autonomous agents. Each agent operates independently, pursuing its own objectives and making decisions based on its individual constraints and capabilities. This decentralized, agent-based approach replaces centralized system planning with self-optimized behavior at the unit level. The model outputs include, among others, plant dispatch, cross-border electricity flows, curtailment of variable renewable energy sources, and electricity prices. A comprehensive overview of the model is provided in [44], with example applications found in [45–47]. While PowerACE simulates 15 European market areas, this study focuses specifically on the market prices generated for Germany. The scenario framework is based on TYNDP 2022-NT [48], with the expansion of renewable energy sources adjusted to align with national targets as of 2024. Thus, a scenario is created that assumes a conservative electricity demand trajectory while incorporating the highly ambitious expansion of renewable energy sources. This results in a scenario with rather low day-ahead market prices that serves as a contrast to current (2024) market conditions. The aim is to explore how emerging technologies perform in a future context characterized by high renewable penetration and a moderated demand outlook, which may lead to structurally lower electricity prices compared to today (2024). To maintain consistency in the dataset, missing annual data points are filled through interpolation. The annual demand and the installed generation capacities by technology type are listed in Table A.1. Renewable generation profiles are based on the Pan-European wind and solar time series developed by the Technical University of Denmark in collaboration with ENTSO-E [49], using 2009 as the reference weather year. Fuel costs are derived from forward market prices as of August 31, 2024, and projections from the World Energy Outlook 2023 [2].

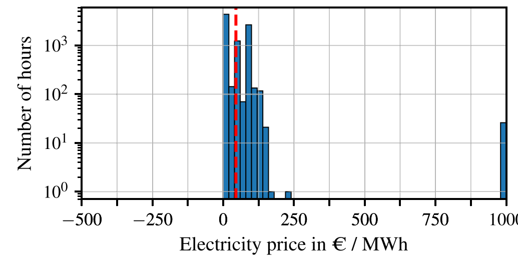

(a) 2030

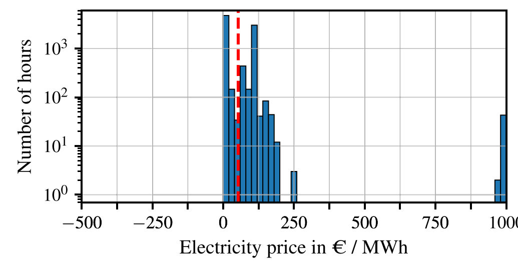

(b) 2035

Fig. 1. Logarithmic histograms of the day-ahead market prices. The average electricity prices of $44.88\,€\,\text{MWh}^{-1}$ in 2030 and $52.99\,€\,\text{MWh}^{-1}$ in 2035 are shown by the red dashed lines. The data originates from the base-case scenario simulated in PowerACE [44].

Fig. 1 shows the logarithmic histograms for the years 2030 and 2035. The underlying data originates from the base-case scenario described above, which was simulated in PowerACE. Negative prices no longer occur, as renewables are modeled to enter the market at zero cost and are curtailed based on market signals, as subsidies are not represented. At the same time, the number of hours with prices close to or equal to $0\,€\,\text{MWh}^{-1}$ increases significantly. In contrast to the historical prices, no distribution resembling a normal distribution is visible; instead, three price levels in 2030 and two price levels in 2035 dominate the distribution. The average electricity price, indicated by the red dashed line, rises from $44.88\,€\,\text{MWh}^{-1}$ in 2030 to $52.99\,€\,\text{MWh}^{-1}$ in 2035, with both values below the two historical average electricity prices under consideration. The standard deviation increases from $65.33\,€\,\text{MWh}^{-1}$ to $83.49\,€\,\text{MWh}^{-1}$ in the same period and is therefore above the historical values. Consequently, the relative standard deviations of the two future electricity price time series are higher than the historical ones. Relative standard deviations of 145.56 % and 157.54 % are achieved for 2030 and 2035.

2.5. LTES unit PEC calculation

When calculating the PEC of the LTES unit, a distinction is made between the three components PCM, finned tubes and tank according to the following equation:

$$PEC_{\text{LTES}} = PEC_{\text{PCM}} + PEC_{\text{tubes}} + PEC_{\text{tank}} \tag{9}$$

For the assumed geometry presented below, these three components cover the main costs of an LTES unit. In a prototype with this design, these three cost components and the manifolds accounted for 85 % of the costs [28]. A further 11 % was attributable to insulation [28], the cost share of which is likely to decrease in larger systems due to an increasing ratio of volume to surface area.

Both the geometry and the required storage capacity are important for selecting the resulting PCM.

Table 2
Fin geometry parameters and values in mm.

$r_{HTF,i}$	$r_{HTF,o}$	r_{PCM}	l_{PCM}	l_{fin}
5	6	50	10	1

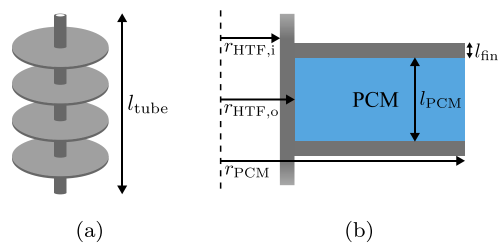

Fig. 2. Geometry of a single tube (a) and cross section view of a single tube section (b)

2.5.1. LTES unit geometry

The basic shape of the LTES unit is assumed to be cylindrical. Heat exchanger tubes are located inside the LTES unit, creating a shell-and-tube heat exchanger structure. The height of the LTES unit and each tube is assumed to be 6 m, which corresponds to the tube length of the German Aerospace Center's LTES unit prototype [33]. The shape of a single finned tube is assumed to be cylindrical and to have the geometry presented in [50], which is based on the hexagonal fin geometry of Laing et al. [51]. An illustration is shown in Fig. 2. For dimensioning purposes, it is assumed that the PCM is only located between the fins. The geometry of the tube is particularly relevant for the cost estimation concerning the PCM volume per tube and thus the required number of tubes.

2.5.2. LTES unit dimensioning

The LTES unit is dimensioned by calculating the thermal storage capacity of a tube and scaling the number of tubes to achieve the required total thermal storage capacity. The thermal storage capacity of a single finned tube C_{tube} is calculated using Eq. (10), whereby only the PCM is taken into account:

$$C_{tube} = h_{PC} \cdot \rho_{PCM} \cdot V_{PCM,tube} \tag{10}$$

where h_{PC} is the enthalpy of fusion of the PCM, ρ_{PCM} is its density and $V_{PCM,tube}$ is the volume it occupies. The latter is determined by:

$$V_{PCM,tube} = \pi \cdot (r_{PCM}^2 - r_{HTF,o}^2) \cdot l_{tube} \cdot \frac{l_{PCM}}{l_{PCM} + l_{fin}} \tag{11}$$

The parameters and values used can be seen in Fig. 2(b) and Table 2. The end faces of the tubes, where another fin would be located, were neglected when calculating the volume. Finally, the required number of tubes is calculated according to:

$$n_{tubes} = \frac{P_{char} \cdot COP \cdot E/P\text{-}ratio}{C_{tube}} \tag{12}$$

Although, in practice, only an integer number of tubes is possible, the number of tubes was not rounded to an integer, as this would result in unintended influence of the length of a single tube.

The COP is varied, whereby its values are specified. As the COP is related to the phase change temperature of the PCM T_{PC}, each temperature can be assigned to a COP for a given exergetic efficiency of the HP $\eta_{ex,HP}$. The following relationship applies between the COP and the phase change temperature of the PCM:

$$T_{PC} = \frac{COP \cdot T_{source}}{COP - \eta_{ex,HP}} \tag{13}$$

This equation results directly from rearranging the expression:

$$COP = \eta_{ex,HP} \cdot COP_{ideal} = \eta_{ex,HP} \cdot \frac{T_{PC}}{T_{PC} - T_{source}} \tag{14}$$

For the source temperature T_{source}, the average temperature in Germany of 283.75 K from the year 2023 is used, which corresponds to 10.6 °C [52].

The exergetic efficiency of the HP varies depending on the round-trip efficiency. Assuming that storage losses can be neglected, the round-trip efficiency depends exclusively on the exergetic efficiency of the HP and the exergetic efficiency of the HE. Their product forms the round-trip efficiency:

$$\eta_{rt} = \eta_{ex,HP} \cdot \eta_{ex,HE} \tag{15}$$

Based on the assumption that the exergetic efficiencies have the same values, the following relationship applies:

$$\eta_{ex,HP} = \eta_{ex,HE} = \sqrt{\eta_{rt}} \tag{16}$$

Consequently, the corresponding phase change temperatures of the PCMs are derived on the basis of the predefined COPs and round-trip efficiencies. For the round-trip efficiencies, values between 30 %, which corresponds to a value in the lower range of the already proven possible round-trip efficiencies [53], and 70 %, which is only slightly below a round-trip efficiency of 72.8 % of a PTES based on several storage units and high isentropic efficiencies of the machines [54], were selected. The COPs and the resulting phase change temperatures considered in this study are summarized in Table 3.

2.5.3. PCM properties and prices

The PCMs considered in this study and their properties are shown in Table 4. The prices of the same PCMs are collected in Table 5. Prices were taken from trading platforms and manufacturers [55–57]. Of the prices researched, the minimum price was used in each case. This is justified by the fact that the requirements for the quality (e.g. purity) of the PCMs are considered to be low.

In order to verify the prices found, some of them are compared with historical prices from the literature. For this purpose, both the time offset through the use of the Chemical Engineering Plant Cost Index (CEPCI) is applied and, if necessary, a correction of the currency using the average exchange rate of 1.36 USD £$^{-1}$ from 2016 [58]. Based on [59], a CEPCI of 540 is estimated for 2016. A CEPCI of 800 is assumed for 2024.

The price comparison is made on the basis of the relative price deviation and is shown in Fig. 3. The difference between the price from the present study in $ kWh^{-1} and the literature value of the price in relation to the former is shown on the abscissa:

$$Relative\ price\ deviation = \frac{p_{study} - p_{lit}}{p_{study}} \tag{17}$$

Values less than zero mean that the literature value is higher. The green dotted vertical lines delimit the range within which there is a deviation of 50 %. The yellow lines delimit the range in which there is a 100 % deviation. The horizontal bars are colored accordingly. It is clear that the majority of PCM prices show a deviation of less than 50 % compared to the literature values. Clear deviations can be seen for urea, which is the main component in some of the PCMs considered, and for high-density polyethylene (HDPE). In the case of HDPE, this is due to the fact that prices of recycled HDPE were used in the present study.

Since various effects such as subcooling, thermal stability and corrosion could limit the application of PCMs, but could be at least partially overcome by appropriate measures [81], all listed PCMs are considered, even if the applicability has not yet been proven.

Table 3
T_{PC} in °C depending on round-trip efficiency and COP.

Round-trip efficiency	COP = 2.25	COP = 2.50	COP = 2.75	COP = 3.00	COP = 3.25	COP = 3.50
0.30	101.90	90.21	81.17	73.98	68.11	63.24
0.35	111.82	98.56	88.37	80.30	73.75	68.32
0.40	121.55	106.69	95.35	86.40	79.16	73.18
0.45	131.13	114.66	102.15	92.32	84.40	77.88
0.50	140.64	122.51	108.81	98.11	89.50	82.44
0.55	150.11	130.28	115.38	103.78	94.49	86.89
0.60	159.57	137.99	121.86	109.36	99.39	91.25
0.65	169.05	145.66	128.29	114.88	104.21	95.52
0.70	178.57	153.33	134.68	120.34	108.97	99.74

Table 4
PCM compositions, abbreviations and physical properties.

PCM main component	PCM additive	wt% additive	Abbreviation	T_{PC} °C	h_{PC} kJ kg^{-1}	$\rho_{PCM,s}$ kg m^{-3}	Sources
Beeswax	Graphene	0.05	–	62.05	156.98	960	[60,61]
Beeswax	Graphene	0.3	BW03	62.42	188.76	960	[60,61]
Stearic acid	Acetamide	17	–	65	213	972	[62]
Magnesium nitrate hexahydrate	Lithium nitrate	14	MNHLN	72	180	1713	[62]
Urea	Lithium nitrate	18	–	76	218	1438	[62]
Barium hydroxide octahydrate	–	–	BHO	78	280	2180	[62,63]
Xylitol (eutectic mixture)	Erythritol	30	–	81.85	270	1272	[64]
Acetamide	–	–	–	82	256.3	1159.5	[62,65,66]
Urea	Sodium nitrate	29	Urea & SN	83	187	1502	[62]
Magnesium nitrate hexahydrate	–	–	MNH	89	151.5	1638	[62,67]
Adonitol	–	–	ADO	98.18	244.5	1530	[64,68,69]
Oxalic acid dihydrate	–	–	OAD	100.25	264	1651.5	[62,70,71]
Urea	Ammonium chloride	15	Urea & AC	102	214	1348	[62]
Potassium carbonate	Urea	15	–	102	206	1415	[62]
Urea	Potassium nitrate	23	–	109	195	1416	[62]
Urea	Sodium chloride	10	Urea & SC	112	230	1372	[62]
Urea	Potassium chloride	11	–	115	227	1370	[62]
Magnesium chloride hexahydrate	–	–	MCH	117	150	1570	[62,72]
Erythritol	–	–	ERY	117.6	340	1418	[62,64,67]
Acetanilide	–	–	–	118.9	180.8	1210	[67,73]
High-density polyethylene	–	–	HDPE	130	222	952	[62,74,75]
Sebacic acid	–	–	SA	131.4	284.5	1210	[76,77]
Potassium nitrate	Lithium nitrate	34	–	133	150	2018	[62]
Potassium nitrate	Sodium nitrite	44	PNSN	141	97	1994	[62]
Sodium nitrate	Potassium nitrite	48	SNPN	149	124	2080	[62]
Adipic acid	–	–	AA	152	255.75	1360	[62,75,78,79]
Lithium nitrate	Sodium nitrite	38	–	156	233	2296	[62]
Lithium nitrate	Potassium chloride	42	–	160	272	2196	[62]
Mannitol	–	–	MAN	162.3	317.85	1505	[62,77,80]
Potassium formate	Sodium formate	45	PFSF	176	175	1913	[62]
Sodium nitrate	Lithium nitrate	49	–	194	262	2317	[62]

2.5.4. PEC of PCM, finned tubes and storage tank

The PEC for the PCM is calculated from the product of the mass-specific price and the mass of PCM:

$$PEC_{\mathrm{PCM}} = p_{\mathrm{PCM}} \cdot m_{\mathrm{PCM}} \tag{18}$$

The price for the finned tubes is set at $p_{\mathrm{tube}} = 10\,\$\,\mathrm{m}^{-1}$. Based on researched prices for finned tubes a wide range of prices was identified. On the one hand, the geometry used is outside the range of commercially available finned tubes [51]. On the other hand, it is assumed that a large order quantity will lead to prices that are usual for commercially finned tubes. Therefore, the selected estimated value can be interpreted as one adapted to the geometry and size of the PTES. The following equation is used to calculate the PEC of the tubes:

$$PEC_{\mathrm{tubes}} = p_{\mathrm{tube}} \cdot l_{\mathrm{tube}} \cdot n_{\mathrm{tubes}} \tag{19}$$

The PEC of the storage tank is calculated according to the correlation of Turton et al. [82] for an API fixed roof tank with the following equation:

$$PEC_{\mathrm{tank}} = 10^{\left(4.8509-0.3973\cdot\log_{10}(A)+0.1445\cdot(\log_{10}(A))^2\right)}\,\$ \tag{20}$$

where A is the capacity parameter, which is used in the unit m^3 and is calculated as follows:

$$A = \pi \cdot r_{\mathrm{PCM}}^2 \cdot l_{\mathrm{tube}} \cdot n_{\mathrm{tubes}} \tag{21}$$

A temporal adjustment is necessary, for which the CEPCI is applied. A value of 397 taken from [82] is used here for the time of the correlation.

2.6. PCM selection

The PEC of the LTES unit depends on the choice of PCM. In addition, only a subset of the PCMs considered can be deployed for each storage temperature. When selecting the PCM, only those are considered whose phase change temperature deviates by up to 5 K from the temperature level associated with the COP and round-trip efficiency or, if the corresponding value is higher, would be equivalent to a deviation in the COP of up to 3 % to allow for a larger temperature interval, especially at higher temperatures. Specifying a temperature range is necessary to ensure that a selection of a PCM remains possible within the scope of this study. The PEC of the LTES unit is determined for each of the remaining PCMs and the PCM that results in the lowest PEC of the LTES unit is selected. Since the prices of the PCMs are mass-specific, but the number of pipes required depends on the volume occupied by the PCM, the most cost-effective PCM does not necessarily provide the lowest PEC of an LTES unit. In addition, the volume of the storage tank depends on the total volume, whose PEC follows a degressive curve and thus takes economies of scale into account. It should be noted at this

Table 5
PCM prices and literature comparison. "+" for PCMs selected by the algorithm, "-" for PCMs not selected by the algorithm, "∘" for PCMs not considered by the algorithm due to their phase change temperature.

PCM	min mass spec. price $/t	Sources of the prices	min energy spec. price $/kWh	Literature price comparison	Selected by the algorithm
Beeswax - Graphene (0.05 %)	600	[55]	13.76	–	–
Beeswax - Graphene (0.3 %)	600	[55]	11.44	–	+
Stearic acid - Acetamide	1134.5	[55,56]	19.17	Fig. 3	–
MNHLN	863.4	[55,56]	17.27	Fig. 3	+
Urea - Lithium nitrate	1064	[55,56]	17.57	Fig. 3	–
BHO	750	[55]	9.64	Fig. 3	+
Xylitol (eutectic mixture) - ERY	2155	[55]	28.73	–	–
Acetamide	3500	[55]	49.16	Fig. 3	–
Urea - Sodium nitrate	374	[55,57]	7.20	Fig. 3	+
MNH	190	[55]	4.51	Fig. 3	+
ADO	15 000	[55]	220.86	–	+
OAD	300	[55]	4.09	Fig. 3	+
Urea - Ammonium chloride	185.45	[55,57]	3.12	Fig. 3	+
Potassium carbonate - Urea	667.5	[55]	11.67	–	–
Urea - Potassium nitrate	338	[55]	6.24	Fig. 3	–
Urea - Sodium chloride	360.71	[55]	5.65	Fig. 3	+
Urea - Potassium chloride	223.1	[55,57]	3.54	Fig. 3	–
MCH	110	[55]	2.60	Fig. 3	+
ERY	1350	14.29	[55]	Fig. 3	+
Acetanilide	1100	[55]	21.90	–	–
HDPE	200	[56]	3.02	Fig. 3	–
SA	500	[55]	6.33	–	+
Potassium nitrate - Lithium nitrate	2228	[55,56]	53.47	Fig. 3	–
PNSN	602	[55]	22.34	Fig. 3	+
SNPN	992	[55,57]	28.80	–	+
AA	900	[56]	12.67	Fig. 3	+
Lithium nitrate - Sodium nitrite	3233	[55,56]	49.95	Fig. 3	–
Lithium nitrate - Potassium chloride	3072.2	[56,57]	40.66	Fig. 3	–
MAN	2000	[55]	22.65	Fig. 3	+
PFSF	599.5	[55,56]	12.33	Fig. 3	+
Sodium nitrate - Lithium nitrate	2858	[55,56]	39.27	Fig. 3	∘

point that the storage tank is the only component in this study whose specific PEC is dependent on size. Since all other assumed costs and also the CM that can be generated on the market increase proportionally with the power of the PTES, the results presented in this study can also be approximately transferred to different sizes of PTESs as long as the price-taker assumption applies. Table 5 shows whether a PCM was selected by the algorithm. This is discussed again in the results section.

2.7. LCOS calculation

The levelized cost of storage (LCOS) are calculated based on [84], neglecting reinvestment costs, and profits or costs for decommissioning and recovery:

$$LCOS = \frac{CAPEX + \sum_{n=1}^{n_E} \left(\frac{OPEX_n + p_{char} \cdot P_{char} \cdot t_{char}}{(1+i)^n} \right)}{\sum_{n=1}^{n_E} \left(\frac{P_{char} \cdot f_P \cdot t_{dis} \cdot \eta_{rt}}{(1+i)^n} \right)} \tag{22}$$

where n is the operating year of the plant, operational expenditure (OPEX) is the annual cost of operating the plant, p_{char} is the average price during the charge process, t_{char} and t_{dis} are the number of hours per year in which the electrical energy storage is charged and discharged, respectively, and i is the interest rate. For the OPEX a value of 3 % of the capital expenditure (CAPEX) is used [85], which only takes maintenance into account. A value of 25 years is assumed as the system lifetime n_E [86]. The interest rate i, which corresponds to weighted average cost of capital (WACC), is set to a value of 8 % [84,87]. The remaining values originate from the simulation.

The calculation of the capital cost, which is assumed to be identical to CAPEX in this study, is carried out according to Towler and Sinnott [59]. The PEC_{tot} and a Lang factor f_{Lang} of 4.74 from the 1940s, which is to be employed for fluid processing plants, are used. Applying the Lang factor allows for a simple estimation of the capital cost based on the PEC of the major equipment, whereby uncertainties of ± 30 % can typically be assumed [59]. The Lang factor for fluid processing plants for 2007 shows only a slight deviation with a value of 4.5 [88], which is why the selected Lang factor can be classified as conservative and still applicable. Furthermore, a location factor for Germany $f_{Germany}$, which takes the value 1.11 for the year 2003 [59], as well as the corresponding average exchange rate $EXR_{€,USD}$ from 2003, which is approximately 0.884 € $^{-1}$ [89], are used:

$$CAPEX = PEC_{tot} \cdot f_{Lang} \cdot f_{Germany} \cdot EXR_{€,USD} \tag{23}$$

The total PEC can be further subdivided into power-related $PEC_{HP,HE}$ and capacity-related PEC_{LTES}:

$$PEC_{tot} = PEC_{HP,HE} + PEC_{LTES} \tag{24}$$

Values between 1 M$ and 6 M$ with an increment of 1 M$ are assumed for the power-related PEC for the system under consideration, which has an electrical input power of 5 MW. They correspond to a specific power-related PEC from 200 € kW^{-1} to 1200 € kW^{-1}. Based on the study of Koksharov et al. [90], a PTES with an input power of 18 MW results in a specific power-related PEC of 675 € kW^{-1} to 1340 € kW^{-1} for the entire PTES, including the costs of the storage unit. Since the power of this PTES is of a similar order of magnitude to that of the system under investigation, the comparable specific PEC is an indicator of their suitable choice. In view of the fact that, according to the formula of Turton et al. [82], two compressors with a capacity of 2.5 MW each, i.e. a total of 5 MW, result in a PEC of slightly more than 1 M$, the lower limit appears optimistic. Nevertheless, such a low specific power-related PEC is considered in the present study, as future, possibly lower-cost PTESs can thus also be taken into account in the context of this investigation.

2.8. Price gap calculation

In order to be able to make a statement about whether a PTES can meet the required WACC or not, the LCOS must be compared

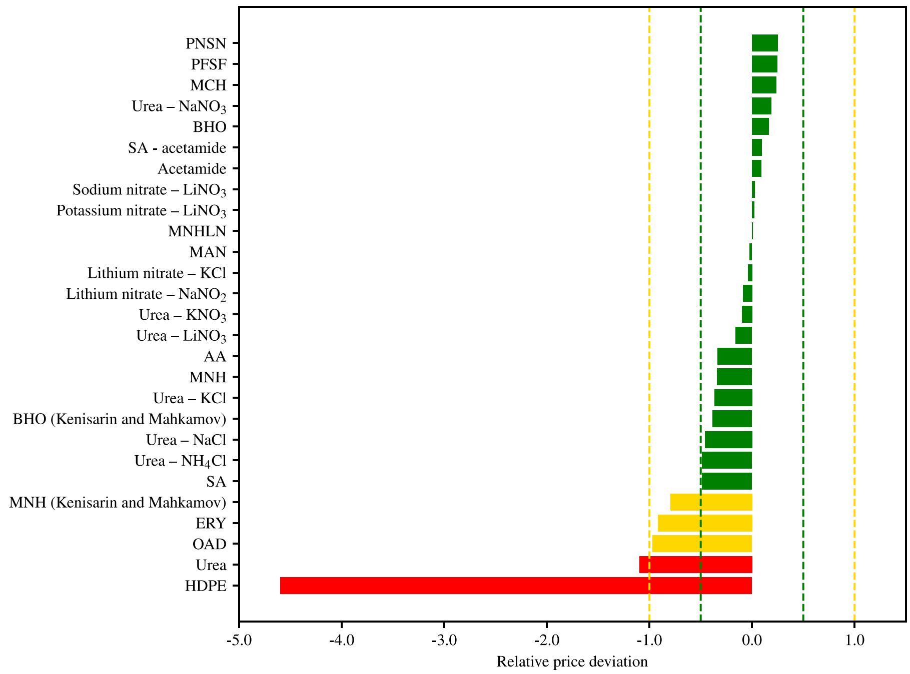

Fig. 3. Relative price deviations. The calculation is done by dividing the difference between the price of the present study in $\$\,kWh^{-1}$ and the literature price (of Da Pereira Cunha and Eames [62] as well as Kenisarin and Mahkamov [83]) by the former. Green dotted lines: 50 % relative deviation; yellow dotted lines: 100 % relative deviation.

with the actual price at which the PTES is discharged. For this reason, the difference between the LCOS and the average discharge price is calculated for the evaluation and is referred to as p_{gap}:

$$p_{gap} = LCOS - p_{dis} \tag{25}$$

The average discharge price required for this originates from the optimization. Negative price gaps indicate that a configuration enables an economically attractive operation.

3. Results and discussion

In order to present the results, the PEC of the LTES unit is discussed first. This can be considered independently of the CM achievable on the market.

Since the power-related PEC is varied according to Table 1, only the parameters round-trip efficiency, E/P-ratio and COP, as listed in Section 2.1, remain as influencing variables for the total PEC, in that they affect the PEC of the LTES unit. Their influence is dealt with in Section 3.1.

The variables influencing the CM are then looked at, where the choice of $R_{char,dis}$ is explained (Section 3.2) and then the handling of the initial state of charge is described (Section 3.3). Next, the influence of the round-trip efficiency and the E/P-ratio on the CM and price gaps is discussed (Section 3.4), whereupon the costs and the CM are summarized by looking at the price gaps for different time series and the influence of all parameters investigated (Sections 3.5 and 3.6). Finally, a parameter study is presented (Section 3.7).

3.1. Capacity-dependent PEC

The PEC of the LTES unit and thus the capacity-dependent share of the PEC depends on the E/P-ratio, the COP and, due to the influence on the selection of the PCM, also on the round-trip efficiency. This allows the PEC to be calculated independently of the CM and therefore does not depend on the year under investigation. The PCMs used as a function of the parameters mentioned are shown in Table 6. These are also marked in Table 5. Since both the required mass of PCM and the number of tubes scale linearly with an increase in E/P-ratio and only the tank of the LTES unit has a non-linear effect, the latter could cause an influence of the E/P-ratio on the choice of the PCM. This is not the case with the present results.

The applicability range of the cost correlation for the tank is slightly undercut for the two PCMs lithium nitrate with sodium nitrite and lithium nitrate with potassium chloride at an E/P-ratio of 1 h. Since the optimal E/P-ratios for the combination of η_{rt} of 60 % and a COP of 2.25, for which the aforementioned PCMs come into question, deviate significantly from an E/P-ratio of 1 h, the applicability of the cost correlation of the tank is guaranteed in the context of this study.

The only two PCMs selected by the algorithm for which the reliability of the price estimate cannot be ensured either by comparison with Fig. 3 or by the existence of a similarly low price are sodium nitrate with potassium nitrite (SNPN) and beeswax with 0.3 % graphene (BW03). Consequently, the assumed prices could be too optimistic. Both occur only once each (see Table 6).

In order to investigate the influence of the price of the finned tubes on the choice of the PCMs, prices of $0\,\$\,m^{-1}$, $5\,\$\,m^{-1}$ and $15\,\$\,m^{-1}$ were used. $0\,\$\,m^{-1}$ represents the economic limit case, in which the impact of the PCM prices is most pronounced. The resulting selected PCMs are shown in Table A.2, A.3 and A.4, with the PCMs in bold highlighting a deviation from the case with $10\,\$\,m^{-1}$.

3.2. Contribution margin – halved discharging duration

By reducing the discharging duration, PTESs can make better use of price peaks. A halving of the discharging duration is therefore compared with the case of the same charging and discharging duration. Fig. 4 shows the relative increase in the achievable CM for the year 2023 with a SoC_0 of 0 h.

With an E/P-ratio of 1 h, the CM does not change, as the halved discharging duration has no impact on the discharge hour used, but only leads to faster discharge in the same hour. Starting at an E/P-ratio of 2 h, a higher CM can be achieved with halved discharging duration, since the PTES can again use the same discharge hour instead of having to fall back on the second-best discharge hour. The difference becomes

Table 6
PCMs selected by the algorithm for $p_{tube} = 10\,\$\,m^{-1}$.

Round-trip efficiency	COP = 2.25	COP = 2.50	COP = 2.75	COP = 3.00	COP = 3.25	COP = 3.50
0.30	OAD	MNH	BHO	BHO	MNHLN	BW03
0.35	Urea & SC	OAD	MNH	BHO	BHO	MNHLN
0.40	ERY	Urea & AC	OAD	MNH	BHO	BHO
0.45	SA	Urea & SC	OAD	MNH	MNH	BHO
0.50	PNSN	ERY	Urea & SC	OAD	MNH	BHO
0.55	AA	SA	Urea & SC	OAD	ADO	MNH
0.60	MAN	PNSN	ERY	Urea & SC	OAD	MNH
0.65	PFSF	SNPN	SA	Urea & SC	OAD	OAD
0.70	PFSF	AA	SA	ERY	Urea & SC	OAD

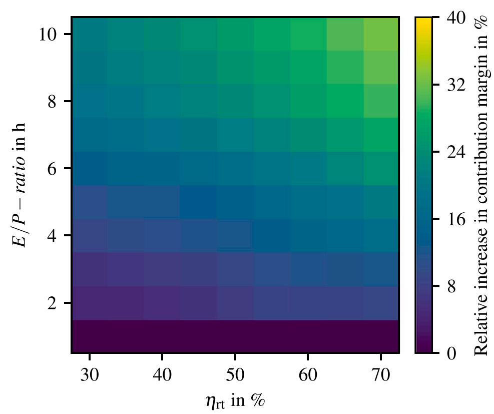

Fig. 4. Relative increase in contribution margin by halving the discharging duration for the year 2023 with a SoC_0 of 0 h.

more apparent as the E/P-ratio increases. In addition, a magnifying influence of increasing round-trip efficiency is discernible. In the results from Section 3.4 onwards, only the results with halved discharging duration are taken into account, as these lead to a higher CM and thus to lower LCOS, so that the limit of an economically attractive operation of PTESs can be more closely approximated.

At this point, it should be emphasized that implementing such a half discharge duration involves technical challenges. In order to double the heat flow from the LTES unit during HE operation compared to the heat flow fed into it during HP operation, larger temperature differences, higher mass flows, or a combination of both are required. The low thermal conductivities of PCMs [68,83,91] can be a limiting factor in heat transfer. The option that is less dependent on sufficiently effective heat transfer is to increase the temperature difference. However, this leads to exergy losses, which makes it difficult to achieve the upper range of round-trip efficiencies examined in this study.

3.3. Contribution margin – initial state of charge

The initial state of charge has an influence on the achievable CM within the optimization, as price peaks in the first hours of the day remain unused if the LTES unit is fully discharged at the beginning of the day or low prices cannot be exploited if the LTES unit is fully charged at this time. The optimal SoC_0 for the year 2023 with equal charging and discharging duration is shown in Fig. 5(a). It becomes clear that the optimal SoC_0 depends on the E/P-ratio. The maximum optimal value of the SoC_0 is 2 h. The percentage storage level to which this corresponds depends on the E/P-ratio under consideration. The relative increase in the CM compared to the case where the SoC_0 is set to 0 h for each optimization can be seen in Fig. 5(b). In the case of the same charging and discharging duration, an identical CM is achieved for E/P-ratios up to 5 h, as the SoC_0 of 0 h corresponds to the optimal solution. With increasing E/P-ratio, the achievable CM increases by up to almost 9 % if the optimal SoC_0 is used instead of the SoC_0 of 0 h. Unless otherwise stated, the results in the following are used with the optimal SoC_0 in each case.

3.4. Contribution margin and p_{gap} – round-trip efficiency and E/P-ratio

The influence of the round-trip efficiency and the E/P-ratio is discussed qualitatively using the example shown in Figs. 6 and 7 for the year 2023. Both Figures show a 3D and 2D representation of the results. The SoC_0 is 0 h. While Fig. 6 shows the achievable CM, Fig. 7 illustrates the price gaps for a power-related PEC of $1M and a COP of 2.5.

It can be observed that in this case the achievable CM increases progressively with increasing round-trip efficiency. Two effects come into play when the round-trip efficiency increases. On the one hand, the CM increases in the hours that could already be used profitably at lower round-trip efficiencies. On the other hand, additional hours can be used profitably. The dependence of the CM shows the same trend in the results based on the future time series but no such pronounced progressive behavior.

With regard to the E/P-ratio, a degressive increase can be seen. The achievable CM asymptotically approaches a round-trip efficiency-dependent threshold. It becomes clear that the benefit of increasing the E/P-ratio decreases as the E/P-ratio increases.

The corresponding price gaps in Fig. 7 show an opposing trend. As the CM increases, the price gap decreases with higher round-trip efficiencies. The minimum price gaps for a given round-trip efficiency are obtained at different E/P-ratios. In this example, the minimum price gaps are achieved at E/P-ratios from 4 h to 6 h, which is highlighted by the red circles. Unlike the CM, the price gaps do not show a monotonic trend. Although the PEC of the LTES unit rises with increasing E/P-ratio, it varies depending on the round-trip efficiency and the associated PCM used.

3.5. p_{gap} – historical prices

Fig. 8 shows the results of the price gaps based on the electricity price time series from 2023. The scale extends to 100 €cent kWh^{-1} to make it easier to compare the values below. In addition, above this value, the distance to economically attractive operation is very large, so it is assumed that knowing the value more precisely does not increase the informative value. The power-related PEC increases from top to bottom and the COP increases from left to right. The results for each combination are displayed in a 2D matrix. Due to the interaction of the round-trip efficiency, the COP and the PCM, no generally valid dependency of the E/P-ratio on one of the parameters mentioned can be determined. As the power-related PEC rises, the price gaps also widens and the PTES becomes increasingly uneconomical. The optimal E/P-ratio for the least uneconomical configuration increases. This is due to the fact that a higher power-related PEC makes a higher capacity-related PEC advantageous, as the higher LTES unit capacity can generate a higher CM, which can reduce the overall electricity-specific costs that correspond to the LCOS.

The lowest optimal E/P-ratio of 2 h was found for a COP of 3.25, the lowest power-related PEC of $1M and adonitol as PCM. As can be seen from the figure, the price gap is strikingly large in this case, which is related to the fact that only the expensive adonitol is available for the selected temperature level. Therefore, an increase in E/P-ratio is more associated with rising PEC of the LTES unit than with other PCMs,

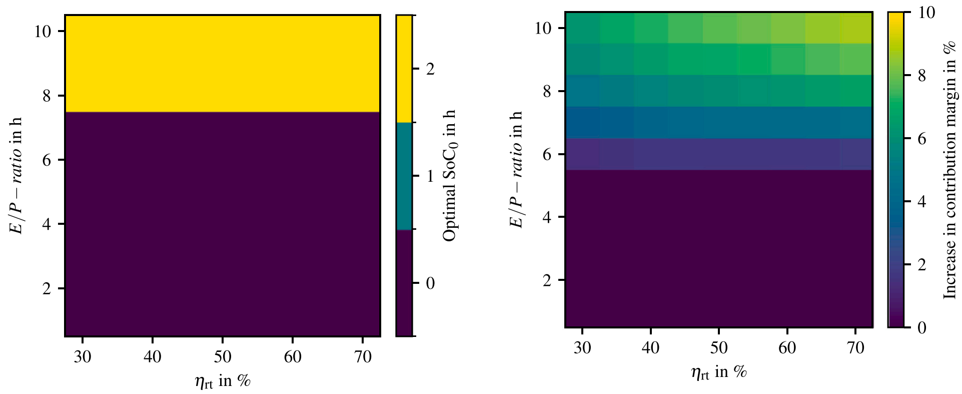

(a) Optimal SoC_0

(b) Increase in the contribution margin when using the optimal SoC_0 compared to the SoC_0 of 0 h

Fig. 5. Influence of SoC_0 for the year 2023 with equal charging and discharging duration. Optimal SoC_0 (a) and increase in the contribution margin when using the optimal SoC_0 compared to the SoC_0 of 0 h (b)

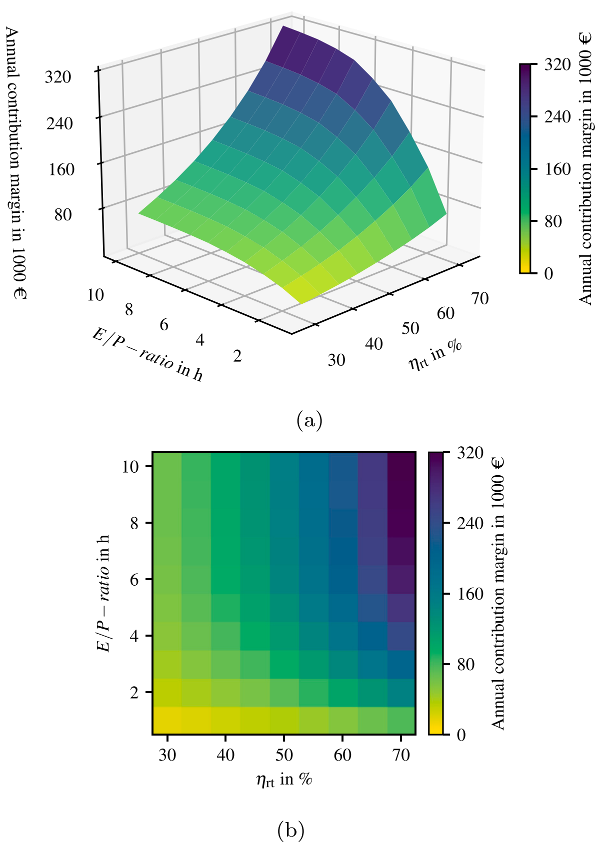

Fig. 6. 3D (a) and 2D (b) illustration of the annual contribution margin with a SoC_0 of 0 h for the year 2023.

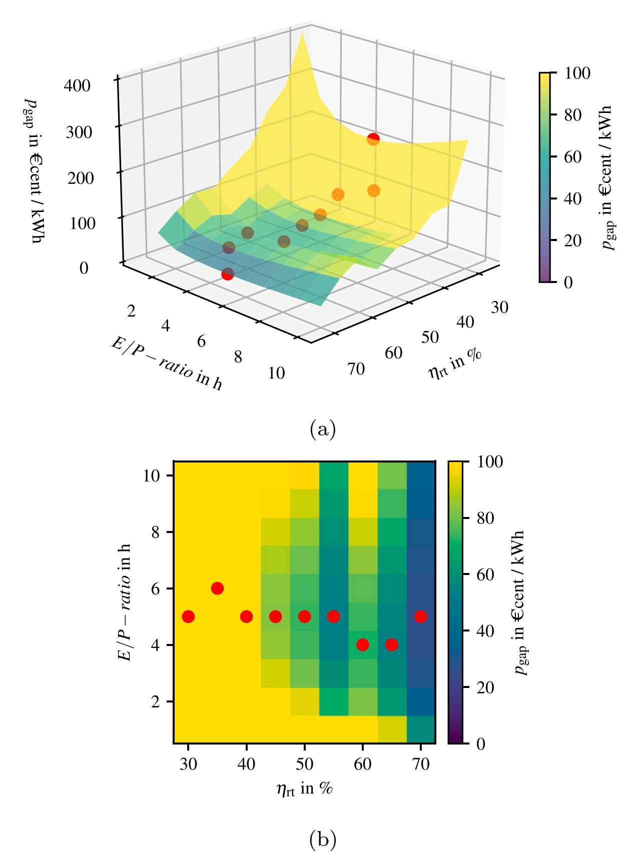

Fig. 7. 3D (a) and 2D (b) illustration of the price gaps with a SoC_0 of 0 h, power-related PEC of $1M, and a COP of 2.5 for the year 2023. The E/P-ratios with the minimum price gaps are highlighted by the red circles.

which is why a particularly low value can be observed here. This makes apparent that the presence of a low-cost PCM is a necessary prerequisite for the economic operation of a PTES based on an LTES unit. Although no configuration allows for economically attractive operation, the price difference resulting from the use of adonitol as opposed to other PCMs allows this conclusion to be drawn. Leaving this special case aside, an optimal E/P-ratio of 4 h is the lowest value. The highest optimal E/P-ratio of 9 h can only be observed for a high power-related PEC and low COPs.

From Fig. 8 it is clear that none of the cases enables a PTES to be operated on the condition that the required WACC is met. This can be seen from the fact that no price gap is negative. The minimum value of the price gap of 23.2 €cent kWh^{-1} is achieved with a COP of 3.5, a power-related PEC of $1M, an E/P-ratio of 5 h and a round-trip efficiency of 70 %. For all COPs, the price gaps for the optimal E/P-ratios and for a round-trip efficiency of 70 % are less than 29 €cent kWh^{-1}, keeping the power-related PEC at $1M.

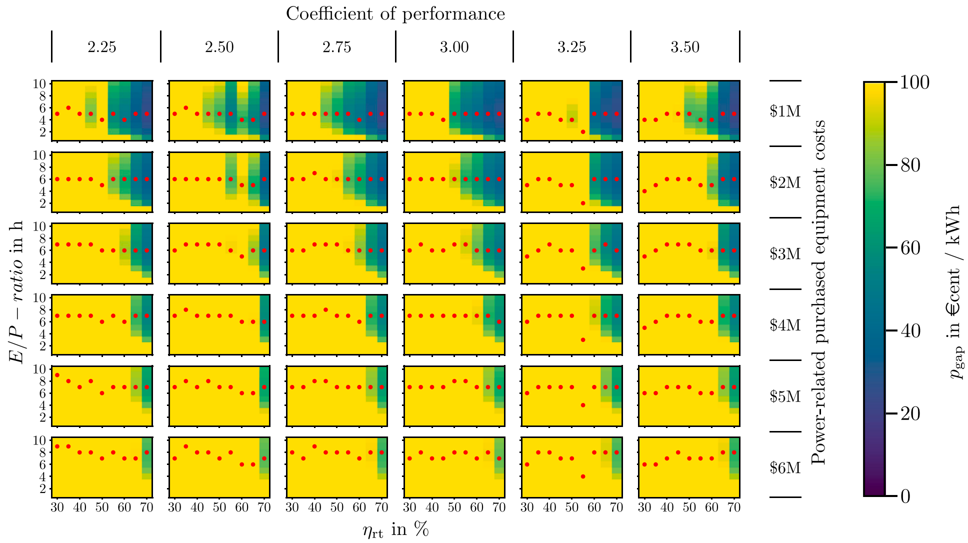

Fig. 8. Price gaps for the year 2023. Outer labeling: COP increases from left to right (2.25, 2.50, 2.75, 3.00, 3.25, 3.50). Power-related purchased equipment cost increases from top to bottom ($1M, $2M, $3M, $4M, $5M, $6M). Inner labeling: E/P-ratio increases from bottom to top (1–10 h) and round-trip efficiency increases from left to right (30–70 %). The E/P-ratios with the minimum price gaps are highlighted by the red circles.

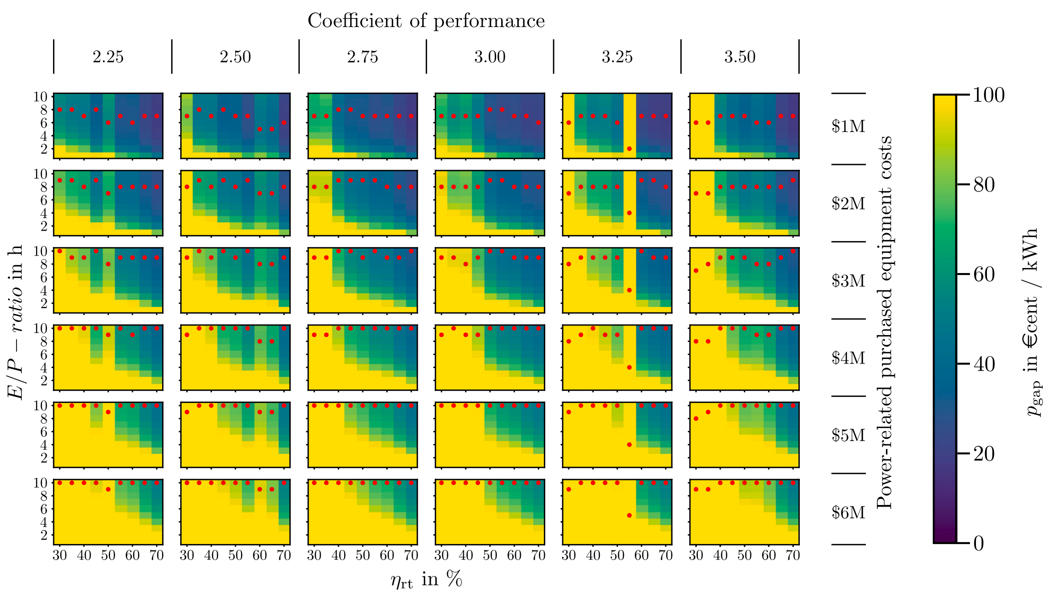

Fig. 9. Price gaps for the year 2030. Outer labeling: COP increases from left to right (2.25, 2.50, 2.75, 3.00, 3.25, 3.50). Power-related purchased equipment cost increases from top to bottom ($1M, $2M, $3M, $4M, $5M, $6M). Inner labeling: E/P-ratio increases from bottom to top (1–10 h) and round-trip efficiency increases from left to right (30–70 %). The E/P-ratios with the minimum price gaps are highlighted by the red circles.

For all power-related PEC considered, the configurations with a round-trip efficiency of 70 %, a COP of 3.5 and oxalic acid dihydrate (OAD) as PCM show the smallest price gaps. The configurations with the same round-trip efficiency and a COP of 2.75, in which sebacic acid is used as PCM, perform second best in terms of achievable price gaps. In both cases, the optimal E/P-ratio varies between 5 h and 8 h. For each round-trip efficiency, the configuration that uses OAD as PCM shows the smallest price gaps.

Since the cost structure is independent of the CM generated, all the observations described above regarding the most favorable PCMs remain valid for all other electricity price time series. OAD can therefore be classified as a potentially promising PCM. In this context, it must be kept in mind that the price for OAD used for this study is significantly lower than the price found in the literature. However, several offers for OAD were found in a similar price range, which increases the significance of the results. Even if the literature price for OAD, which is nearly twice as high as the price used in this study, is assumed, this would have only a limited impact on the choice of the PCMs. In the cases where the price of the finned tubes is $0\,\$\,m^{-1}$, $10\,\$\,m^{-1}$, and $15\,\$\,m^{-1}$, the results remain unchanged. In the case of $5\,\$\,m^{-1}$, OAD is replaced by urea & AC in the eight cases where it is also replaced at $0\,\$\,m^{-1}$ for the prices used in this study. The use of urea & AC instead of OAD thus shifts toward higher prices of the finned tubes. Furthermore, configurations using OAD no longer have the smallest price gaps for every round-trip efficiency. In most cases, configurations using sebacic acid or urea & SC show the smallest price gaps instead of those with OAD. It should be kept in mind that the assumed prices for both sebacic acid and urea are also significantly lower than those taken from the literature. Therefore, despite this finding, OAD is still considered promising from an economic point of view.

Lower achievable price gaps are present for the year 2024 (see Fig. A.2). The minimum is 18.8 €cent kWh^{-1} for a round-trip efficiency of

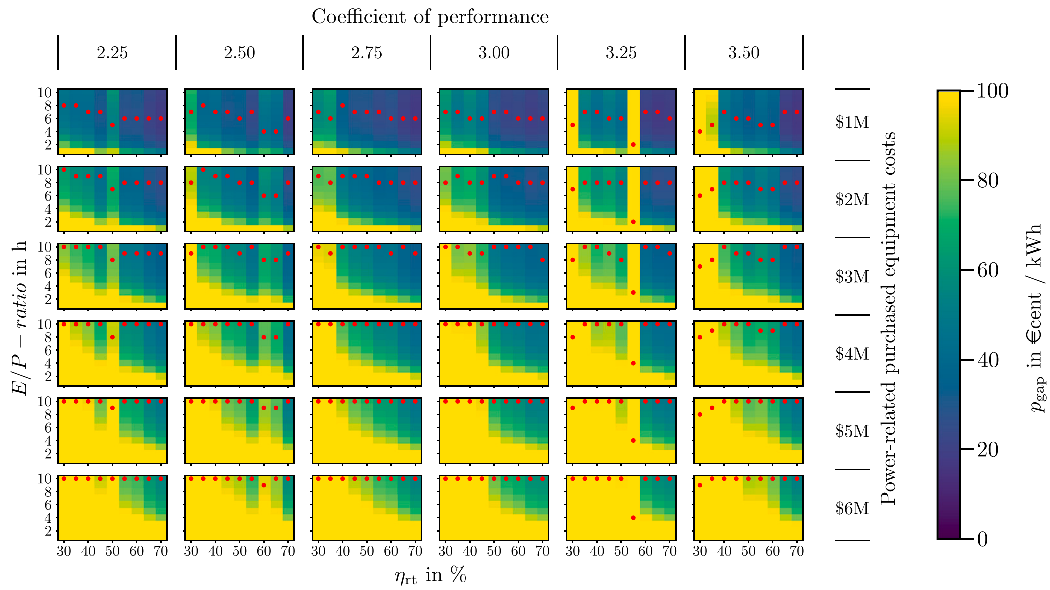

Fig. 10. Price gaps for the year 2035. Outer labeling: COP increases from left to right (2.25, 2.50, 2.75, 3.00, 3.25, 3.50). Power-related purchased equipment cost increases from top to bottom ($1M, $2M, $3M, $4M, $5M, $6M). Inner labeling: E/P-ratio increases from bottom to top (1–10 h) and round-trip efficiency increases from left to right (30–70 %). The E/P-ratios with the minimum price gaps are highlighted by the red circles.

70 % and a COP of 3.5 for a minimum power-related PEC, with OAD again selected as PCM. This is in line with the expectations from the analyses from Section 2.3, according to which higher relative standard deviations lead to a higher CM, resulting in lower price gaps.

3.6. p_{gap} – future prices

As far as future price gaps are concerned, the price gaps drop to minimum values of 17.1 €cent kWh^{-1} in 2030 (Fig. 9) and 16.5 €cent kWh^{-1} in 2035 (Fig. 10) for an optimal E/P-ratio of 7 h. It is noticeable that the price gaps also fall below 100 €cent kWh^{-1} for higher power-related PEC. In addition, the assumed electricity price structure appears to lead to a partial reduction in the discrepancy between high and low round-trip efficiencies. Furthermore, it can be seen that higher E/P-ratios are more advantageous. There is no optimal E/P-ratio for 2030 that is less than 5 h and none for 2035 that is less than 4 h. The optimal E/P-ratios even reach the limit of the parameter range investigated, which makes it seem likely that in some cases even higher E/P-ratios than 10 h would represent the most economical configuration. It should be kept in mind that the PTES does not have to be operated for 20 h to utilize this E/P-ratio, as the discharging duration is only half the charging duration. Furthermore, with an E/P-ratio of 10 h, it is possible for the PTES to be operated for more than 15 h if storage capacity is used several times during the day.

However, even with future electricity prices, no configuration of a PTES results in an operation that ensures the demanded WACC.

3.7. Parameter study of future electricity prices

In order to evaluate the influence of future electricity prices, a parameter study was carried out. Four variants of the scenario for the year 2035 were considered. In addition, the impact of changes in the Lang factor and in the WACC were examined.

The renewable energy capacity was varied to 80 % and 120 % of the base-case scenario (Figs. A.3 and A.4) and the fuel prices were changed to 80 % and 120 % of the base-case scenario in PowerACE (Figs. A.5 and A.6). Both the base-case and the 120 % renewable energy capacity case have consistently optimal E/P-ratios that are greater than or equal to that of the 80 % renewable energy capacity case. However, it is observed that the price gaps decrease for most configurations in the 80 % renewable energy capacity case, while they increase in the 120 % case. For the fuel prices, the majority of the optimal E/P-ratios are identical, but this is partly due to the fact that more than half of the optimal E/P-ratios have the value 10 h. None of the scenarios shows the possibility of economically attractive operation with any configuration.

To assess whether the results obtained would be fundamentally altered by less conservative assumptions in the cost calculation, two more optimistic cost estimates are additionally presented for the base-case scenario of the year 2035. First, a Lang factor for solid-fluid processing plants for the year 2007 of 3.5 [88] will be considered, which is slightly below the value of 3.63 given in [82] from the 1940s. Second, a required WACC of 6 % is examined.

The results are shown in Fig. A.7 for the reduced Lang factor and in Fig. A.8 for the reduced WACC. It becomes clear that, despite the reduction in price gaps down to 9.5 €cent kWh^{-1} and 13.1 €cent kWh^{-1}, respectively, economically viable operation is not possible. Even a combination of both measures would not result in negative price gaps for the base-case scenario of the year 2035.

4. Uncertainties and restrictions

Various aspects should be taken into account when interpreting the results and are therefore discussed in the following.

When calculating the LCOS, estimates are made for the OPEX, the interest rate, and the service life of the PTES, which could deviate in a real plant. The calculation of CAPEX based on the Lang factor, which also affects the LCOS, is another source of uncertainty. CAPEX, for its part, is based on the prices of PCMs, which, as can be seen by comparing them with literature prices, may show significant deviations in some cases.

On the market side, the amount of the grid fee is subject to uncertainty. The modeling approach, which assumes perfect foresight but also limits energy storage to one day, represents a considerable simplification. E/P-ratios of more than 16 h, which corresponds to the theoretical limit of the E/P-ratio for one day, although only those up to 10 h were investigated, could thus generate an additional CM. According to the results of Connolly et al. [20], a daily perfect forecast with an E/P-ratio comparable to those in the present study can achieve about 97 % of the optimal profits that could be obtained with the optimization on an annual basis. The results of Lund et al. [23] show that 80 %–90 % of the optimal CM can be expected in real operation. Although these two studies do not deal with the German electricity market, they help to assess the reliability of the results of the present study for the E/P-ratios investigated. With respect to PowerACE, the scenario simulated represents only one possible development pathway. Given the large number of parameters influencing future electricity price trajectories, a broader range of scenarios should be examined to derive robust conclusions, particularly as the parameter study revealed that a scenario with lower renewable energy capacity represents a more favorable starting point for most configurations.

PTESs do not appear to meet the required WACC without subsidies, even for the highest round-trip efficiency of 70 % examined and a very low power-related PEC, provided that only the exploitation of price spreads is considered to generate a CM. Changes in the assumptions listed above make an economically attractive operation conceivable. The fact that electrical energy storage cannot be operated economically in Germany through the exclusive use of price spreads is in line with the results of Zakeri et al. [27], although this study is based on time series from around 10 years ago, which limits comparability.

The results allow to derive an initial tendency regarding the economic viability of PTES in other markets on the basis of the average value and standard deviation of electricity prices. However, a reliable transferability to other markets does not exist, as is also evident from cross-national studies [18,20]. One reason for this is that a country-specific cost factor f_{Germany} was used. However, what is much more decisive is that the electricity price time series originate from the German electricity market or, in the case of future electricity market prices, were created explicitly for this market.

Other markets, such as the reserve markets, and cost savings, such as the cost reduction of industrial companies through peak load capping, could offer further financial benefits. Also to be considered in the context of industrial companies are opportunities for waste heat utilization and heat sales, which are also not the subject of this study. If existing infrastructures or only plant components, such as HPs, HEs, LTES units or subsystems thereof, for example compressors or heat exchangers, could be used, this would be another way of reducing costs and thus achieving economically attractive operation of PTESs.

Technological limitations must also be taken into account. In a real-world system, it is not possible to start up and shut down the PTES instantly due to thermal and mechanical inertia. This causes deviations from ideal behavior and thus has a negative impact on the economic viability of a PTES. Another challenge in the context of PCMs is their long-term stability during cyclic operation [92], which is also not considered in the present study. A limited cyclic stability could shorten the system lifetime of the PTES or necessitate a reinvestment in new PCM.

Furthermore, this study takes an exclusively economic perspective and does not take into account other aspects such as supply risk or political motivations for diversifying energy storage systems.

5. Conclusion

In this study, the optimal E/P-ratios of LTES unit based PTESs were determined for historical price time series and future electricity price time series derived from a scenario with highly ambitious renewable energy expansion. For this purpose, an optimization was performed on a daily basis with perfect foresight. The German electricity market is the market under investigation. In addition to the electricity price time series, the influence of round-trip efficiency, COP, power-related purchased equipment cost, ratio between charging and discharging duration and initial state of charge was investigated.

First, the most cost-effective LTES unit configurations and the associated PCMs were identified. Furthermore, it was found that an increased ratio between charging and discharging duration has a positive influence on the achievable contribution margin on the market, which is reinforced with increasing round-trip efficiency. In addition, depending on the E/P-ratio, a partially filled storage unit at the beginning of the day can lead to a higher achievable contribution margin. Both the increase in round-trip efficiency and the E/P-ratio lead to a rising contribution margin.

For the year 2023, the smallest price gap of 23.2 €cent kWh^{-1} was identified with a COP of 3.5, a power-related purchased equipment cost of \$1M and an E/P-ratio of 5 h. Looking at the year 2024, this difference is still 18.8 €cent kWh^{-1} for an E/P-ratio of 6 h, all other parameters being equal. It should be emphasized that these configurations are hypothetical, so the feasibility of their implementation is not guaranteed. It is also important to note that the values given here regarding price gaps and E/P-ratios are not universally applicable, but depend on the assumptions made in this study. As the combination of round-trip efficiency, COP and PCM results in individual configurations, their combined influence does not lead to a shift in the optimal E/P-ratio.

Oxalic acid dihydrate resulted in the most cost-effective LTES unit configurations for all efficiencies considered. Oxalic acid dihydrate, with a melting temperature of about 100 °C, is therefore seen as a promising PCM for LTES unit based PTESs from an economic point of view. However, technical parameters relevant to real-world implementation, such as the thermal conductivity and cyclic stability of PCMs, were not taken into account in their evaluation. The necessity of the existence of a low-cost PCM for the operation of such PTESs was demonstrated by the high-priced adonitol in this study. Apart from this outlier, optimal E/P-ratios of at least 4 h are obtained for both historical and future electricity price time series. A rising power-related purchased equipment cost results in an increase in the optimal E/P-ratio.

For the electricity price time series derived from an agent-based model within a high renewable share scenario, price gaps are decreasing, bringing the PTES closer to economically attractive operation, even with higher power-related purchased equipment cost and lower round-trip efficiencies. However, as with historical prices, economically attractive operation is still not achievable on the German electricity market within the given scenarios. Nevertheless, it can be observed that the optimal E/P-ratio shifts to higher values within the future scenario with lower electricity market prices and higher relative standard deviations in the electricity price time series. This also applies under varied conditions with regard to the expansion of renewable energy capacity and fuel prices, as was shown by a parameter study. Furthermore, neither a reduction in the Lang factor nor in the required WACC resulted in an economically attractive operation. It should be noted in particular that only the use of price spreads to generate a contribution margin was considered in the present study. Other financial benefits such as a contribution margin from trading on reserve markets or reductions in expenditure for companies due to peak load capping are not included. In addition, neither the use of waste heat nor the sale of heat are taken into account, which means that potential for efficiency benefits and other achievable contribution margins are not considered.

It would therefore be desirable to estimate the economically optimal E/P-ratios based on an energy system model, taking into account the aforementioned influences that increase the economic viability of PTESs.

CRediT authorship contribution statement

Lauritz Zendel: Writing – review & editing, Writing – original draft, Visualization, Validation, Software, Methodology, Investigation, Formal analysis, Data curation, Conceptualization. **Jonathan Stelzer:** Writing – review & editing, Writing – original draft, Validation, Software, Data curation. **Frank Dammel:** Writing – review & editing, Supervision, Methodology. **Wolf Fichtner:** Writing – review & editing, Supervision, Resources, Project administration, Funding acquisition. **Peter Stephan:** Writing – review & editing, Supervision, Resources, Project administration, Funding acquisition.

Declaration of Generative AI and AI-assisted technologies in the writing process

During the preparation of this work the authors used DeepL and ChatGPT in order to improve language and readability. After using these tools, the authors reviewed and edited the content as needed and take full responsibility for the content of the publication.

Declaration of competing interest

The authors declare that they have no known competing financial interests or personal relationships that could have appeared to influence the work reported in this paper.

Acknowledgments

Funding by the German Research Foundation within the Priority Programme 2403: 'Carnot-Batteries: Inverse Design from Markets to Molecules' under project numbers 525974553 and 526233915 is gratefully acknowledged. The assistance provided by Fredy Lianggara in researching the properties and prices of phase change materials is gratefully acknowledged.

Appendix

See Figs. A.2–A.8.
See Tables A.1–A.4.

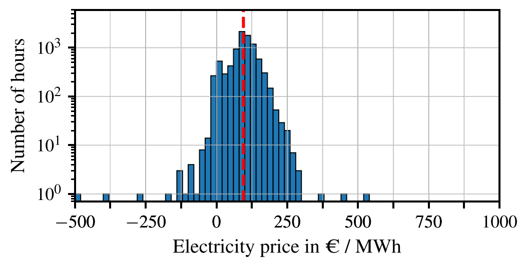

(a) 2023

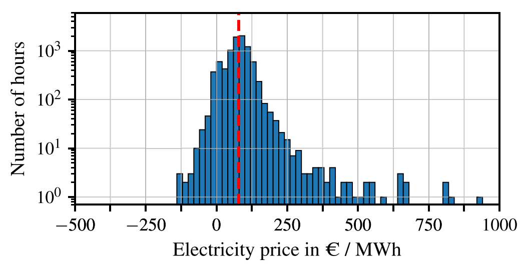

(b) 2024

Fig. A.1. Logarithmic histograms of the day-ahead market prices. The average electricity prices of 95.18 € MWh^{-1} in 2023 and 78.55 € MWh^{-1} in 2024 are shown by the red dashed lines.

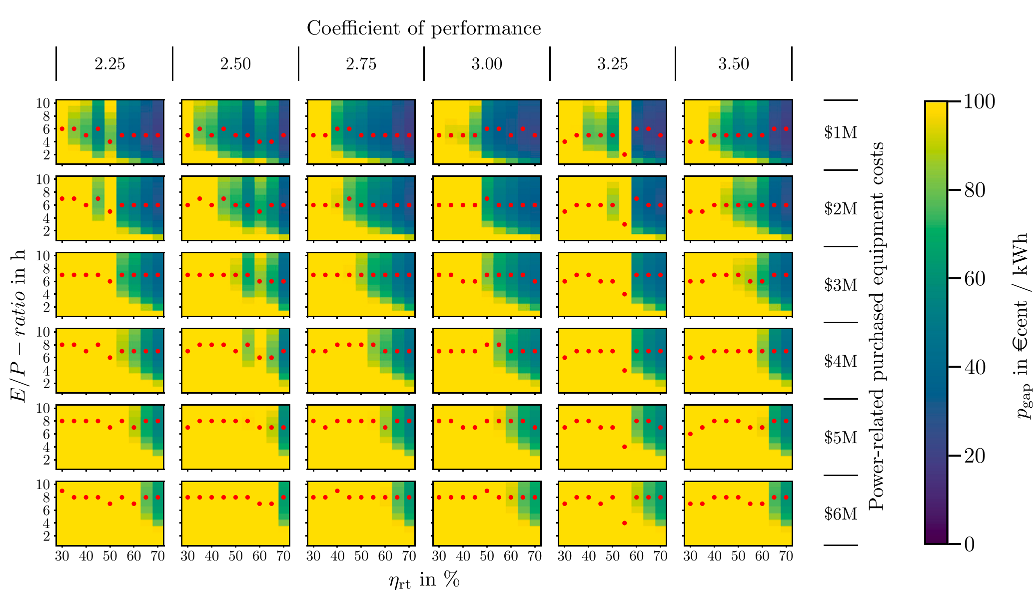

Fig. A.2. Price gaps for the year 2024. Outer labeling: COP increases from left to right (2.25, 2.50, 2.75, 3.00, 3.25, 3.50). Power-related purchased equipment cost increases from top to bottom ($1M, $2M, $3M, $4M, $5M, $6M). Inner labeling: E/P-ratio increases from bottom to top (1–10 h) and round-trip efficiency increases from left to right (30–70 %). The E/P-ratios with the minimum price gaps are highlighted by the red circles.

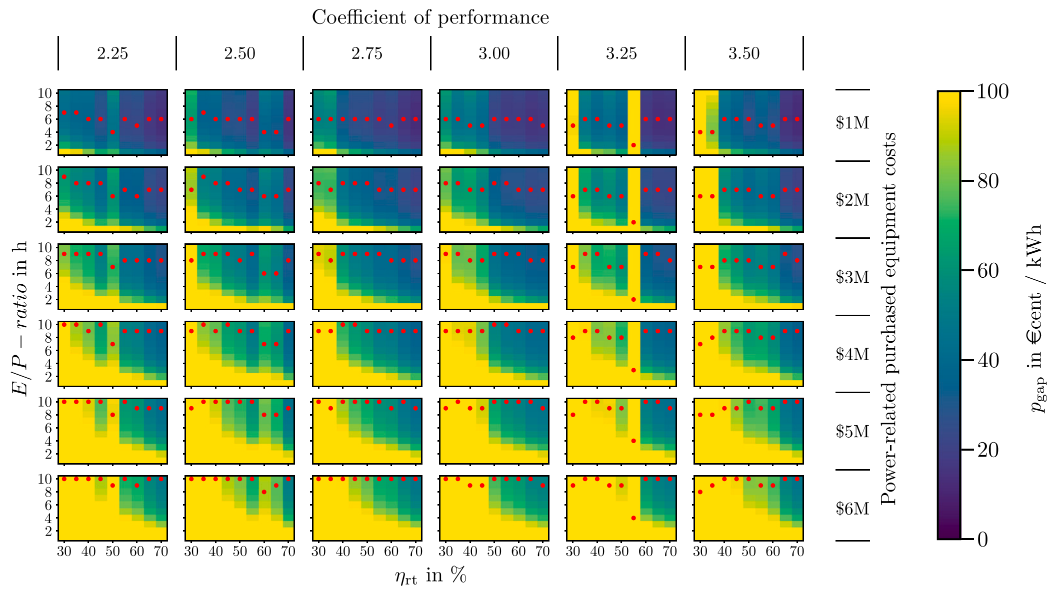

Fig. A.3. Price gaps for the year 2035. Outer labeling: COP increases from left to right (2.25, 2.50, 2.75, 3.00, 3.25, 3.50). Power-related purchased equipment cost increases from top to bottom ($1M, $2M, $3M, $4M, $5M, $6M). Inner labeling: E/P-ratio increases from bottom to top (1–10 h) and round-trip efficiency increases from left to right (30–70 %). The E/P-ratios with the minimum price gaps are highlighted by the red circles. Low renewable energy capacity scenario (80 % renewable energy capacity of the base-case scenario)

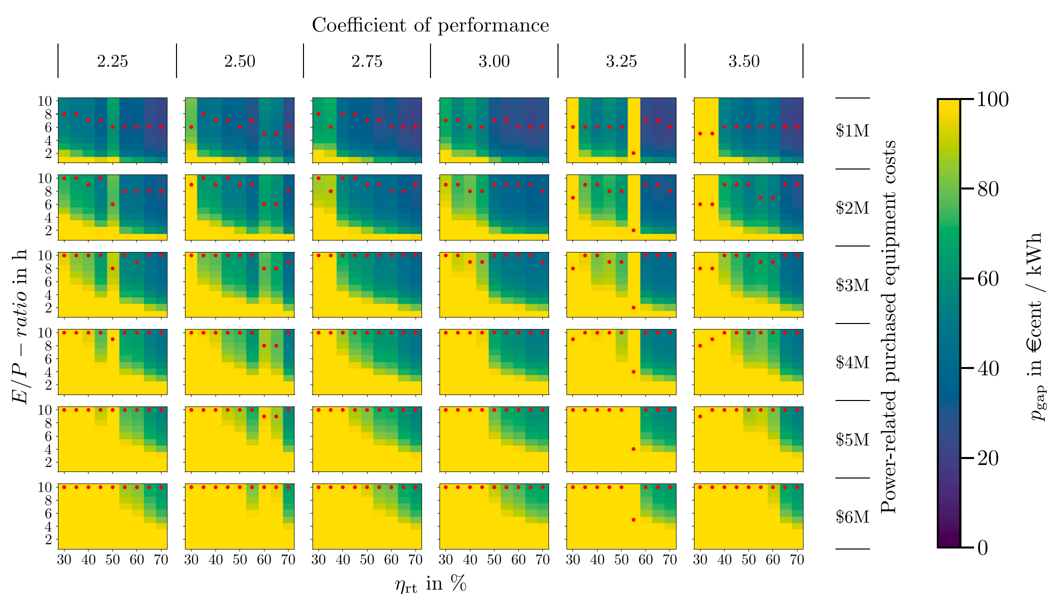

Fig. A.4. Price gaps for the year 2035. Outer labeling: COP increases from left to right (2.25, 2.50, 2.75, 3.00, 3.25, 3.50). Power-related purchased equipment cost increases from top to bottom ($1M, $2M, $3M, $4M, $5M, $6M). Inner labeling: E/P-ratio increases from bottom to top (1–10 h) and round-trip efficiency increases from left to right (30–70 %). The E/P-ratios with the minimum price gaps are highlighted by the red circles. High renewable energy capacity scenario (120 % renewable energy capacity of the base-case scenario)

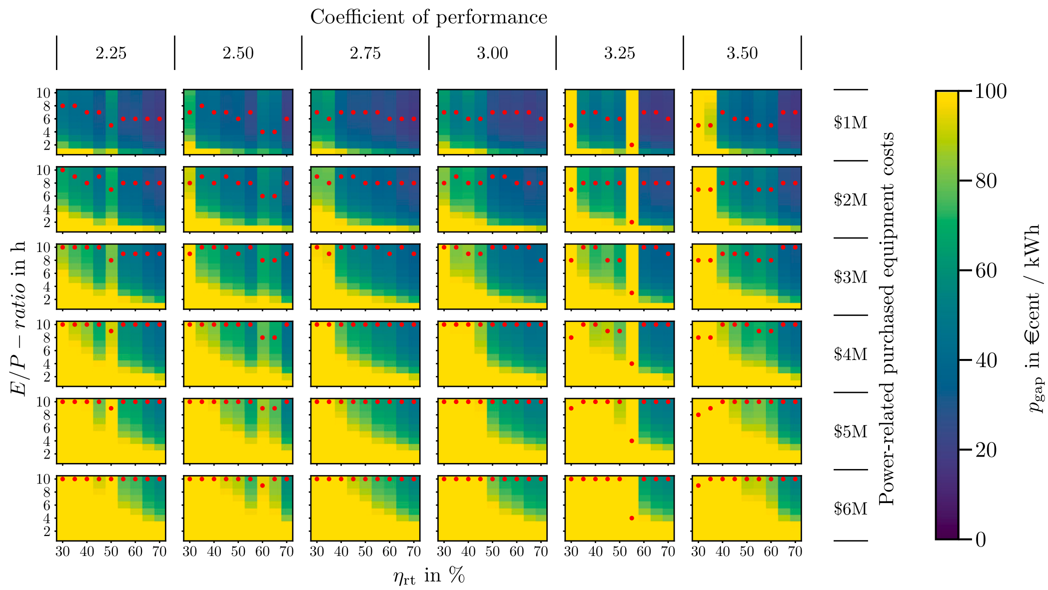

Fig. A.5. Price gaps for the year 2035. Outer labeling: COP increases from left to right (2.25, 2.50, 2.75, 3.00, 3.25, 3.50). Power-related purchased equipment cost increases from top to bottom ($1M, $2M, $3M, $4M, $5M, $6M). Inner labeling: E/P-ratio increases from bottom to top (1–10 h) and round-trip efficiency increases from left to right (30–70 %). The E/P-ratios with the minimum price gaps are highlighted by the red circles. Low fuel prices scenario (80 % fuel prices of the base-case scenario)

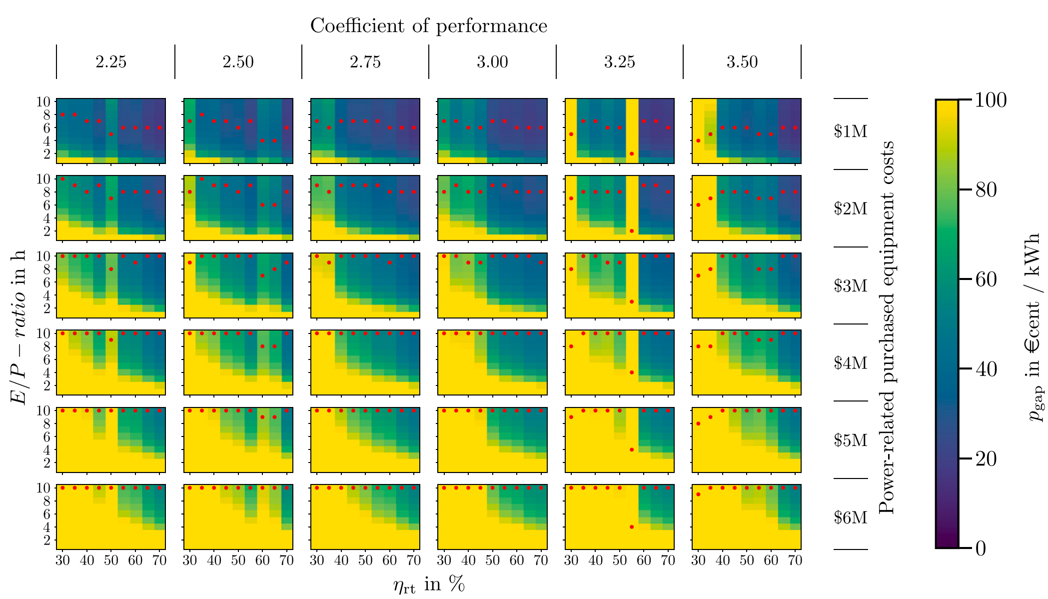

Fig. A.6. Price gaps for the year 2035. Outer labeling: COP increases from left to right (2.25, 2.50, 2.75, 3.00, 3.25, 3.50). Power-related purchased equipment cost increases from top to bottom ($1M, $2M, $3M, $4M, $5M, $6M). Inner labeling: E/P-ratio increases from bottom to top (1–10 h) and round-trip efficiency increases from left to right (30–70 %). The E/P-ratios with the minimum price gaps are highlighted by the red circles. High fuel prices scenario (120 % fuel prices of the base-case scenario)

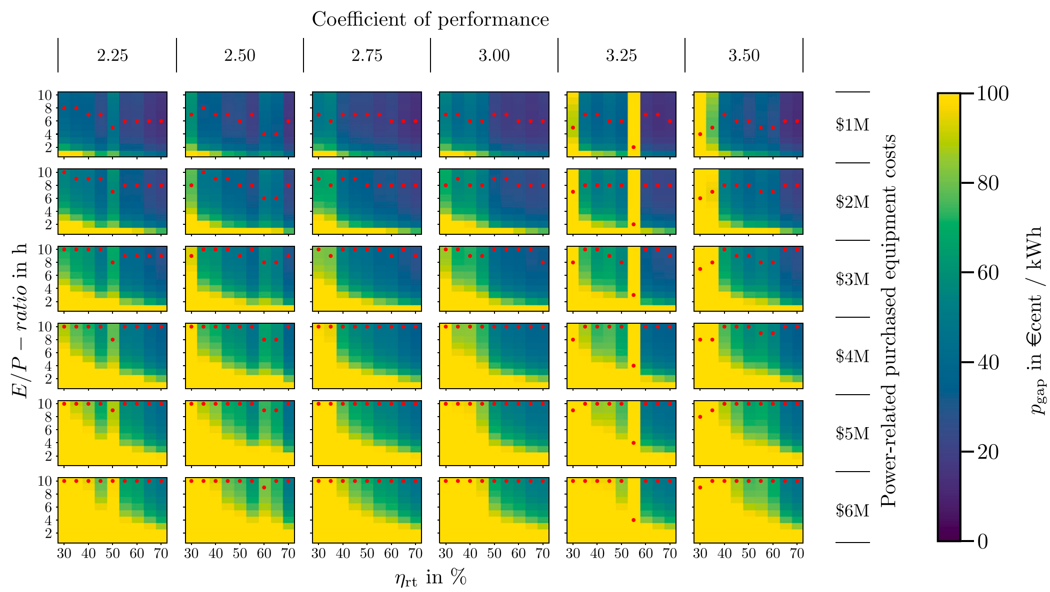

Fig. A.7. Price gaps for the year 2035. Outer labeling: COP increases from left to right (2.25, 2.50, 2.75, 3.00, 3.25, 3.50). Power-related purchased equipment cost increases from top to bottom ($1M, $2M, $3M, $4M, $5M, $6M). Inner labeling: E/P-ratio increases from bottom to top (1–10 h) and round-trip efficiency increases from left to right (30–70 %). The E/P-ratios with the minimum price gaps are highlighted by the red circles. Low Lang factor (f_{Lang} = 3.5) for the base-case scenario.

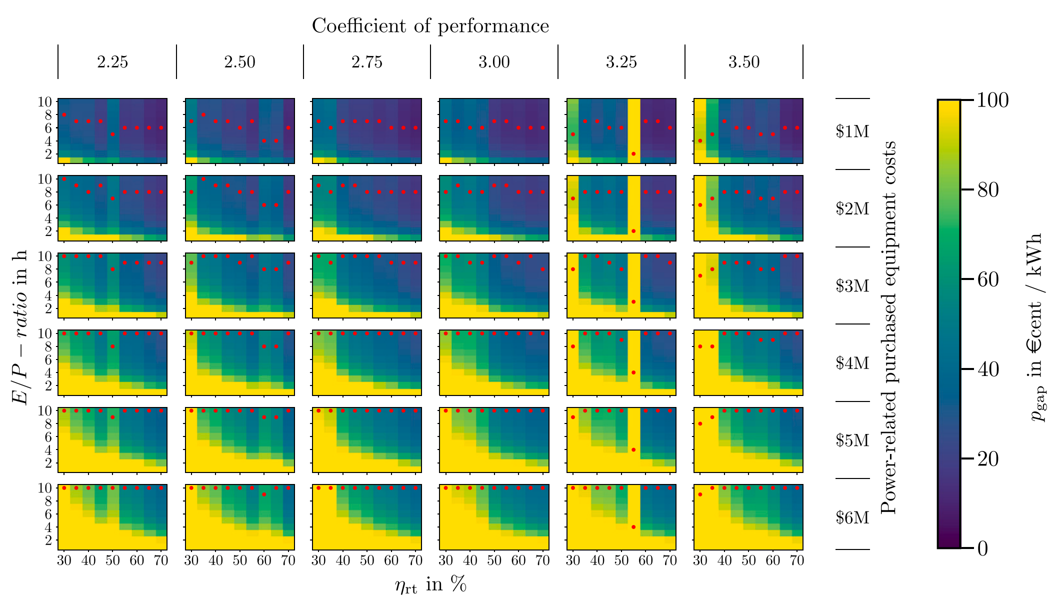

Fig. A.8. Price gaps for the year 2035. Outer labeling: COP increases from left to right (2.25, 2.50, 2.75, 3.00, 3.25, 3.50). Power-related purchased equipment cost increases from top to bottom ($1M, $2M, $3M, $4M, $5M, $6M). Inner labeling: E/P-ratio increases from bottom to top (1–10 h) and round-trip efficiency increases from left to right (30–70 %). The E/P-ratios with the minimum price gaps are highlighted by the red circles. Low WACC (WACC = 6 %) for the base-case scenario.

Table A.1
Annual demand and generation capacities by technology type in Germany used in the PowerACE simulation.

Technology type	2030	2035
Natural gas, oil and hydrogen	29.8 GW	30.9 GW
Run-of-river, hard coal and lignite	32.1 GW	23.7 GW
Wind	145.0 GW	172.0 GW
PV	215.0 GW	307.0 GW
PHES	9.0 GW	9.1 GW
Lithium-ion battery	4.9 GW	6.2 GW
Demand side response	7.4 GW	7.5 GW
Others	17.4 GW	18.6 GW
Annual demand	596.6 TWh	683.9 TWh

Table A.2
PCMs selected by the algorithm for the cost of the finned tubes of 0 € m^{-1}. Entries in bold differ from the case with 10 € m^{-1}.

Round-trip efficiency	COP = 2.25	COP = 2.50	COP = 2.75	COP = 3.00	COP = 3.25	COP = 3.50
0.30	Urea & AC	MNH	Urea & SN	BHO	MNHLN	BW03
0.35	Urea & SC	Urea & AC	MNH	Urea & SN	BHO	MNHLN
0.40	MCH	Urea & AC	OAD	MNH	Urea & SN	BHO
0.45	HDPE	Urea & SC	Urea & AC	MNH	MNH	BHO
0.50	PNSN	ERY	Urea & SC	Urea & AC	MNH	Urea & SN
0.55	AA	HDPE	Urea & SC	Urea & AC	ADO	MNH
0.60	MAN	PNSN	MCH	Urea & SC	Urea & AC	MNH
0.65	PFSF	PNSN	HDPE	Urea & SC	Urea & AC	OAD
0.70	PFSF	AA	HDPE	MCH	Urea & SC	Urea & AC

Table A.3
PCMs selected by the algorithm for the cost of the finned tubes of 5 € m^{-1}. Entries in bold differ from the case with 10 € m^{-1}.

Round-trip efficiency	COP = 2.25	COP = 2.50	COP = 2.75	COP = 3.00	COP = 3.25	COP = 3.50
0.30	OAD	MNH	BHO	BHO	MNHLN	BW03
0.35	Urea & SC	OAD	MNH	BHO	BHO	MNHLN
0.40	MCH	Urea & AC	OAD	MNH	BHO	BHO
0.45	SA	Urea & SC	OAD	MNH	MNH	BHO
0.50	PNSN	ERY	Urea & SC	OAD	MNH	BHO
0.55	AA	SA	Urea & SC	OAD	ADO	MNH
0.60	MAN	PNSN	MCH	Urea & SC	OAD	MNH
0.65	PFSF	PNSN	SA	Urea & SC	OAD	OAD
0.70	PFSF	AA	SA	MCH	Urea & SC	OAD

Table A.4
PCMs selected by the algorithm for the cost of the finned tubes of 15 € m^{-1}. Entries in bold differ from the case with 10 € m^{-1}.

Round-trip efficiency	COP = 2.25	COP = 2.50	COP = 2.75	COP = 3.00	COP = 3.25	COP = 3.50
0.30	OAD	MNH	BHO	BHO	MNHLN	BW03
0.35	Urea & SC	OAD	MNH	BHO	BHO	MNHLN
0.40	ERY	Urea & AC	OAD	Urea & SN	BHO	BHO
0.45	SA	Urea & SC	OAD	MNH	Urea & SN	BHO
0.50	PNSN	ERY	Urea & SC	OAD	MNH	BHO
0.55	AA	SA	Urea & SC	OAD	ADO	Urea & SN
0.60	MAN	PNSN	ERY	Urea & SC	OAD	MNH
0.65	PFSF	SNPN	SA	Urea & SC	OAD	OAD
0.70	PFSF	AA	SA	ERY	Urea & SC	OAD

Data availability

Data will be made available on request.

References

[1] IPCC, Climate Change 2023: Synthesis Report. Contribution of Working Groups I, II and III to the Sixth Assessment Report of the Intergovernmental Panel on Climate Change [Core Writing Team, H. Lee and J. Romero (eds.)], Intergovernmental Panel on Climate Change (IPCC), Geneva, Switzerland, 2023, http://dx.doi.org/10.59327/IPCC/AR6-9789291691647.001.

[2] IEA, World energy outlook 2023: Licence: CC by 4.0 (report); CC by NC sa 4.0 (annex a), 2023, URL https://www.iea.org/reports/world-energy-outlook-2023.

[3] International Energy Agency, Energy Statistics Data Browser - Wind electricity generation, Energy statistics data browser: Wind electricity generation, 2023, URL https://www.iea.org/data-and-statistics/data-tools/energy-statistics-data-browser?country=WORLD&fuel=Renewables%20and%20waste&indicator=WindGen.

[4] IRENA, Renewable Energy Statistics 2023, International Renewable Energy Agency, Abu Dhabi, 2023, URL https://www.irena.org/Publications/2023/Jul/Renewable-energy-statistics-2023.

[5] International Energy Agency, Energy Statistics Data Browser - Solar PV electricity generation, Energy statistics data browser: Solar PV electricity generation, 2023, URL https://www.iea.org/data-and-statistics/data-tools/energy-statistics-data-browser?country=WORLD&fuel=Renewables%20and%20waste&indicator=SolarGen.

[6] IRENA, Tripling Renewable Power and Doubling Energy Efficiency by 2030 Crucial Steps Towards 1.5°C, International Renewable Energy Agency, Conference of the Parties (United Nations Framework Convention on Climate Change), Abu Dhabi, 2023.

[7] IEA, Technology roadmap: Energy storage, 2014, URL https://www.researchgate.net/publication/261848307_Technology_Roadmap_Energy_storage. Organisation for Economic Co-operation and Development and International Energy Agency.

[8] M. Schoenfisch, A. Dasgupta, Grid-scale storage: Technology deployment, 2023, URL https://www.iea.org/energy-system/electricity/grid-scale-storage. International Energy Agency.

[9] A. Vecchi, K. Knobloch, T. Liang, H. Kildahl, A. Sciacovelli, K. Engelbrecht, Y. Li, Y. Ding, Carnot battery development: A review on system performance, applications and commercial state-of-the-art, J. Energy Storage 55 (2022) 105782, http://dx.doi.org/10.1016/j.est.2022.105782.

[10] O. Dumont, G.F. Frate, A. Pillai, S. Lecompte, M. de Paepe, V. Lemort, Carnot battery technology: A state-of-the-art review, J. Energy Storage 32 (2020) 101756, http://dx.doi.org/10.1016/j.est.2020.101756.

[11] A. Benato, A. Stoppato, Pumped thermal electricity storage: A technology overview, Therm. Sci. Eng. Prog. 6 (2018) 301–315, http://dx.doi.org/10.1016/j.tsep.2018.01.017.

[12] K. Attonaty, P. Stouffs, J. Pouvreau, J. Oriol, A. Deydier, Thermodynamic analysis of a 200 MWh electricity storage system based on high temperature thermal energy storage, Energy 172 (2019) 1132–1143, http://dx.doi.org/10.1016/j.energy.2019.01.153.

[13] S. Schmeing, A. Welp, B. Atakan, Experimental investigation of a heat pump coupled to a thermal storage for charging a carnot battery, 2025, http://dx.doi.org/10.36227/techrxiv.176478421.10869135/v1.

[14] M. Albert, Z. Ma, H. Bao, A.P. Roskilly, Operation and performance of Brayton pumped thermal energy storage with additional latent storage, Appl. Energy 312 (2022) 118700, http://dx.doi.org/10.1016/j.apenergy.2022.118700.

[15] X.J. Xue, C.Y. Zhao, Transient behavior and thermodynamic analysis of Brayton-like pumped-thermal electricity storage based on packed-bed latent heat/cold stores, Appl. Energy 329 (2023) 120274, http://dx.doi.org/10.1016/j.apenergy.2022.120274.

[16] F. Nitsch, M. Wetzel, H.C. Gils, K. Nienhaus, The future role of carnot batteries in Central Europe: Combining energy system and market perspective, J. Energy Storage 85 (2024) 110959, http://dx.doi.org/10.1016/j.est.2024.110959.

[17] M. Merten, C. Olk, I. Schoeneberger, D.U. Sauer, Bidding strategy for battery storage systems in the secondary control reserve market, Appl. Energy 268 (2020) 114951, http://dx.doi.org/10.1016/j.apenergy.2020.114951.

[18] T. Mercier, M. Olivier, E. de Jaeger, The value of electricity storage arbitrage on day-ahead markets across Europe, Energy Econ. 123 (2023) 106721, http://dx.doi.org/10.1016/j.eneco.2023.106721.

[19] A. Vecchi, J. Naughton, Y. Li, P. Mancarella, A. Sciacovelli, Multi-mode operation of a liquid air energy storage (LAES) plant providing energy arbitrage and reserve services – analysis of optimal scheduling and sizing through MILP modelling with integrated thermodynamic performance, Energy 200 (2020) 117500, http://dx.doi.org/10.1016/j.energy.2020.117500.

[20] D. Connolly, H. Lund, P. Finn, B.V. Mathiesen, M. Leahy, Practical operation strategies for pumped hydroelectric energy storage (PHES) utilising electricity price arbitrage, Energy Policy 39 (7) (2011) 4189–4196, http://dx.doi.org/10.1016/j.enpol.2011.04.032.

[21] G.F. Frate, L. Ferrari, U. Desideri, Critical review and economic feasibility analysis of electric energy storage technologies suited for grid scale applications, E3S Web Conf. 137 (2019) 01037, http://dx.doi.org/10.1051/e3sconf/201913701037.

[22] G.F. Frate, L. Ferrari, U. Desideri, Energy storage for grid-scale applications: Technology review and economic feasibility analysis, Renew. Energy 163 (2021) 1754–1772, http://dx.doi.org/10.1016/j.renene.2020.10.070.

[23] H. Lund, G. Salgi, B. Elmegaard, A.N. Andersen, Optimal operation strategies of compressed air energy storage (CAES) on electricity spot markets with fluctuating prices, Appl. Therm. Eng. 29 (5–6) (2009) 799–806, http://dx.doi.org/10.1016/j.applthermaleng.2008.05.020.

[24] I. Staffell, M. Rustomji, Maximising the value of electricity storage, J. Energy Storage 8 (2016) 212–225, http://dx.doi.org/10.1016/j.est.2016.08.010.

[25] I. Wilson, E. Barbour, T. Ketelaer, W. Kuckshinrichs, An analysis of storage revenues from the time-shifting of electrical energy in Germany and Great Britain from 2010 to 2016, J. Energy Storage 17 (2018) 446–456, http://dx.doi.org/10.1016/j.est.2018.04.005.

[26] D. Metz, J.T. Saraiva, Use of battery storage systems for price arbitrage operations in the 15- and 60-min German intraday markets, Electr. Power Syst. Res. 160 (2018) 27–36, http://dx.doi.org/10.1016/j.epsr.2018.01.020.

[27] B. Zakeri, S. Syri, F. Wagner, Economics of energy storage in the german electricity and reserve markets, in: 2017 14th International Conference on the European Energy Market, EEM, IEEE, 2017, pp. 1–6, http://dx.doi.org/10.1109/EEM.2017.7981914.

[28] W.D. Steinmann, Thermal Energy Storage for Medium and High Temperatures: Concepts and Applications, Springer Fachmedien Wiesbaden GmbH, Wiesbaden, 2022.

[29] N.I. Ibrahim, F.A. Al-Sulaiman, S. Rahman, B.S. Yilbas, A.Z. Sahin, Heat transfer enhancement of phase change materials for thermal energy storage applications: A critical review, Renew. Sustain. Energy Rev. 74 (2017) 26–50, http://dx.doi.org/10.1016/j.rser.2017.01.169.

[30] H. Kumar, A. Yadav, G. Singh, S. Taneja, A detailed review of the design parameters for augmenting the latent heat in a thermal energy storage system, Energy Harvest. Syst. 12 (1) (2025) http://dx.doi.org/10.1515/EHS-2023-0038.

[31] M. Johnson, J. Vogel, M. Hempel, B. Hachmann, A. Dengel, Design of high temperature thermal energy storage for high power levels, Sustain. Cities Soc. 35 (2017) 758–763, http://dx.doi.org/10.1016/j.scs.2017.09.007.

[32] D. Laing, T. Bauer, D. Lehmann, C. Bahl, Development of a thermal energy storage system for parabolic trough power plants with direct steam generation, J. Sol. Energy Eng. 132 (2) (2010).

[33] D. Laing, T. Bauer, N. Breidenbach, B. Hachmann, M. Johnson, Development of high temperature phase-change-material storages, Appl. Energy 109 (2013) 497–504, http://dx.doi.org/10.1016/j.apenergy.2012.11.063.

[34] T. Pirasaci, D.Y. Goswami, Influence of design on performance of a latent heat storage system for a direct steam generation power plant, Appl. Energy 162 (2016) 644–652, http://dx.doi.org/10.1016/j.apenergy.2015.10.105.

[35] S.S.M. Tehrani, R.A. Taylor, P. Saberi, G. Diarce, Design and feasibility of high temperature shell and tube latent heat thermal energy storage system for solar thermal power plants, Renew. Energy 96 (2016) 120–136, http://dx.doi.org/10.1016/j.renene.2016.04.036.

[36] A.V. Olympios, J.D. McTigue, P. Farres-Antunez, A. Tafone, A. Romagnoli, Y. Li, Y. Ding, W.-D. Steinmann, L. Wang, H. Chen, C.N. Markides, Progress and prospects of thermo-mechanical energy storage—a critical review, Prog. Energy 3 (2) (2021) 022001, http://dx.doi.org/10.1088/2516-1083/abdbba.

[37] B. Lin, W. Wu, M. Bai, C. Xie, J. Radcliffe, Liquid air energy storage: Price arbitrage operations and sizing optimization in the GB real-time electricity market, Energy Econ. 78 (2019) 647–655, http://dx.doi.org/10.1016/j.eneco.2018.11.035.

[38] R. Tassenoy, K. Couvreur, W. Beyne, M.D. Paepe, S. Lecompte, Introduction of a high-level, application based sizing methodology for carnot batteries, in: Proceedings of the 6th International Seminar on ORC Power Systems, 2021, http://dx.doi.org/10.14459/2021mp1633036.

[39] O. Dumont, C. Poletto, O. Thomé, V. Lemort, Methodology for the sizing of a carnot battery based on a rankine cycle and application to a 10 kwe system for district heating application, in: J.R. Smith (Ed.), 36th International Conference on Efficiency, Cost, Optimization, Simulation and Environmental Impact of Energy Systems, ECOS 2023, ECOS 2023, Las Palmas De Gran Canaria, Spain, 2023, pp. 2300–2308, http://dx.doi.org/10.52202/069564-0207.

[40] Bundesnetzagentur and Bundeskartellamt, Monitoringbericht 2023, 2023, URL https://data.bundesnetzagentur.de/Bundesnetzagentur/SharedDocs/Mediathek/Monitoringberichte/MonitoringberichtEnergie2023.pdf.

[41] M.L. Bynum, G.A. Hackebeil, W.E. Hart, C.D. Laird, B.L. Nicholson, J.D. Siirola, J.-P. Watson, D.L. Woodruff, Pyomo - optimization modeling in python, third ed., in: Springer eBook Collection, vol. 67, Springer, Cham, 2021, http://dx.doi.org/10.1007/978-3-030-68928-5.

[42] W.E. Hart, J.-P. Watson, D.L. Woodruff, Pyomo: modeling and solving mathematical programs in python, Math. Program. Comput. 3 (3) (2011) 219–260, http://dx.doi.org/10.1007/s12532-011-0026-8.

[43] Marktdaten: Markt - groß handelspreise - stündliche auflösung, 2024, URL https://www.smard.de/home/downloadcenter/download-marktdaten/. Bundesnetzagentur | SMARD.de.

[44] C. Fraunholz, Market Design for the Transition to Renewable Electricity Systems, Karlsruhe Institute of Technology (KIT), 2021, http://dx.doi.org/10.5445/IR/1000133282.

[45] C. Fraunholz, D. Hladik, D. Keles, D. Möst, W. Fichtner, On the long-term efficiency of market splitting in Germany, Energy Policy 149 (2021) 111833, http://dx.doi.org/10.1016/j.enpol.2020.111833.

[46] T. Signer, N. Baumgartner, M. Ruppert, T. Sandmeier, W. Fichtner, Modeling V2G spot market trading: The impact of charging tariffs on economic viability, Energy Policy 189 (2024) 114109, http://dx.doi.org/10.1016/j.enpol.2024.114109.

[47] F. Zimmermann, A. Bublitz, D. Keles, W. Fichtner, Cross-border effects of capacity remuneration mechanisms: The Swiss case, Energy J. 42 (2) (2021) 53–90, http://dx.doi.org/10.5547/01956574.42.2.fzim.

[48] ENTSO-E, ENTSOG, TYNDP 2022 Scenario Report, ENTSO-E, ENTSOG, 2022, URL https://2022.entsos-tyndp-scenarios.eu/wp-content/uploads/2022/04/TYNDP2022_Joint_Scenario_Full-Report-April-2022.pdf.

[49] M.J. Koivisto, J.P.M. Leon, Pan-European wind and solar generation time series (PECD 2021 update), Technical University of Denmark, 2022, http://dx.doi.org/10.11583/DTU.c.5939581.v3.

[50] A. Dietrich, Assessment of Pumped Heat Electricity Storage Systems through Exergoeconomic Analyses (Ph.D. thesis), Universitäts- und Landesbibliothek Darmstadt, Darmstadt, 2017.

[51] D. Laing, T. Bauer, W.-D. Steinmann, D. Lehmann, Advanced high temperature latent heat storage system - design and test results, in: Effstock 2009, 2009.

[52] Deutschlandwetter im jahr 2023: Erwärmungstrend hält an: 2023 mit neuem rekord und reichlich niederschlag, 2023, URL https://www.dwd.de/DE/presse/pressemitteilungen/DE/2023/20231229_deutschlandwetter_jahr2023_news.html.

[53] V. Novotny, V. Basta, P. Smola, J. Spale, Review of carnot battery technology commercial development, Energies 15 (2) (2022) 647, http://dx.doi.org/10.3390/en15020647.

[54] W.D. Steinmann, The CHEST (compressed heat energy storage) concept for facility scale thermo mechanical energy storage, Energy 69 (2014) 543–552, http://dx.doi.org/10.1016/j.energy.2014.03.049.

[55] Focus Technology Co. Ltd., Made-in-China, Nanjing, Made-in-China. URL https://www.made-in-china.com/?pv_id=1ikufnmgkb96&faw_id=1ikufnog1867,

[56] Alibaba.com Singapore E-Commerce Private Limited, Singapore, Alibaba, 2025, URL https://www.alibaba.com/.

[57] ChemAnalyst, New York, Chemanalyst, 2025, URL https://www.chemanalyst.com/.

[58] Exchange-Rates.org: British Pound (GBP) to US Dollar (USD) Exchange Rate History for 2016. URL https://www.exchange-rates.org/exchange-rate-history/gbp-usd-2016. MBH Media, Inc.

[59] G. Towler, R. Sinnott, Capital cost estimating, in: Chemical Engineering Design, Elsevier, 2022, pp. 239–278.

[60] M. Amin, N. Putra, E.A. Kosasih, E. Prawiro, R.A. Luanto, T. Mahlia, Thermal properties of beeswax/graphene phase change material as energy storage for building applications, Appl. Therm. Eng. 112 (2017) 273–280, http://dx.doi.org/10.1016/j.applthermaleng.2016.10.085.

[61] H.H. Root, Beeswax : Its Properties, Testing, Production and Applications, Chemical Publishing Co., Brooklin, New York, 1951.

[62] J. Da Pereira Cunha, P. Eames, Thermal energy storage for low and medium temperature applications using phase change materials – A review, Appl. Energy 177 (2016) 227–238, http://dx.doi.org/10.1016/j.apenergy.2016.05.097.

[63] Barium hydroxide octahydrate: Properties, 2024, URL https://lab.honeywell.com/shop/barium-hydroxide-octahydrate-31127. Honeywell International Inc.

[64] E.P. Del Barrio, A. Godin, M. Duquesne, J. Daranlot, J. Jolly, W. Alshaer, T. Kouadio, A. Sommier, Characterization of different sugar alcohols as phase change materials for thermal energy storage applications, Sol. Energy Mater. Sol. Cells 159 (2017) 560–569, http://dx.doi.org/10.1016/j.solmat.2016.10.009.

[65] B. Brahma, R. Narzary, D.C. Baruah, Acetamide for latent heat storage: Thermal stability and metal corrosivity with varying thermal cycles, Renew. Energy 145 (2020) 1932–1940, http://dx.doi.org/10.1016/j.renene.2019.07.109.

[66] Merck KGaA. Acetamide: Eigenschaften. Darmstadt, Acetamide: Eigenschaften, 2025, URL https://www.sigmaaldrich.com/DE/de/product/mm/822343?srsltid=AfmBOoop3dOA85ISLLm6QBmbJhRlnKwGFTShHv-KEo7PGcLGx3tpF2bC.

[67] N.H. Abu-Hamdeh, K.A. Alnefaie, Assessment of thermal performance of PCM in latent heat storage system for different applications, Sol. Energy 177 (2019) 317–323, http://dx.doi.org/10.1016/j.solener.2018.11.035.

[68] M.M. Kenisarin, Thermophysical properties of some organic phase change materials for latent heat storage. A review, Sol. Energy 107 (2014) 553–575, http://dx.doi.org/10.1016/j.solener.2014.05.001.

[69] Adonitol, 99.8%, MP biomedicals™: Specifications, 2024, URL https://www.fishersci.fi/shop/products/adonitol-99-8-mp-biomedicals-2/11482910. Thermo Fisher Scientific Inc.
[70] Merck KGaA. Oxalsäure-Dihydrat: Physiochemische Informationen. Darmstadt, Oxalsäure-dihydrat: Physiochemische informationen, 2025, URL https://www.merckmillipore.com/DE/de/product/Oxalic-acid-dihydrate,MDA_CHEM-100489?.
[71] Oxalic acid dihydrate: physical & chemical information, 2021, URL https://chemicalsafety.ilo.org/dyn/icsc/showcard.display?p_version=2&p_card_id=0707. International Labour Organization and World Health Organization.
[72] Merck KGaA. Magnesiumchlorid-Hexahydrat: Physiochemische Informationen. Darmstadt, Magnesiumchlorid-hexahydrat: Physiochemische informationen, 2025, URL https://www.merckmillipore.com/DE/de/product/Magnesium-chloride-hexahydrate,MDA_CHEM-105833?.
[73] A.B. Shobo, A. Mawire, Experimental comparison of the thermal performances of acetanilide, meso-erythritol and an In-Sn alloy in similar spherical capsules, Appl. Therm. Eng. 124 (2017) 871–882, http://dx.doi.org/10.1016/j.applthermaleng.2017.06.091.
[74] D. Haillot, T. Bauer, U. Kröner, R. Tamme, Thermal analysis of phase change materials in the temperature range 120–150°C, Thermochim. Acta 513 (1–2) (2011) 49–59, http://dx.doi.org/10.1016/j.tca.2010.11.011.
[75] A. Mawire, K.A. Lentswe, A. Shobo, Performance comparison of four spherically encapsulated phase change materials for medium temperature domestic applications, J. Energy Storage 23 (2019) 469–479, http://dx.doi.org/10.1016/j.est.2019.04.007.
[76] Sebacic acid: physical & chemical information, 2021, URL https://chemicalsafety.ilo.org/dyn/icsc/showcard.display?p_version=2&p_card_id=1685. International Labour Organization and World Health Organization.
[77] Z. Huang, N. Xie, Z. Luo, X. Gao, X. Fang, Y. Fang, Z. Zhang, Characterization of medium-temperature phase change materials for solar thermal energy storage using temperature history method, Sol. Energy Mater. Sol. Cells 179 (2018) 152–160, http://dx.doi.org/10.1016/j.solmat.2017.11.006.
[78] Adipic acid: physical & chemical information, 2021, URL https://chemicalsafety.ilo.org/dyn/icsc/showcard.display?p_version=2&p_card_id=0369. International Labour Organization and World Health Organization.
[79] Merck KGaA. Adipinsäure: Physiochemische Informationen. Darmstadt, Adipinsäure: Physiochemische informationen, 2025, URL https://www.merckmillipore.com/DE/de/product/Adipic-acid,MDA_CHEM-818650.
[80] Merck KGaA. D(-)-Mannit: Physiochemische Informationen. Darmstadt, D(-)-mannit: Physiochemische informationen, 2025, URL https://www.merckmillipore.com/DE/de/product/D-Mannitol,MDA_CHEM-105982?.
[81] D.S. Jayathunga, H.P. Karunathilake, M. Narayana, S. Witharana, Phase change material (PCM) candidates for latent heat thermal energy storage (LHTES) in concentrated solar power (CSP) based thermal applications - a review, Renew. Sustain. Energy Rev. 189 (2024) 113904, http://dx.doi.org/10.1016/j.rser.2023.113904.
[82] R. Turton, R.C. Bailie, W.B. Whiting, J.A. Shaeiwitz, D. Bhattacharyya, Analysis, synthesis, and design of chemical processes, fourth ed., in: Prentice Hall International Series in the Physical and Chemical Engineering Sciences, Prentice Hall, Upper Saddle River, N.J. and Munich, 2012.
[83] M. Kenisarin, K. Mahkamov, Salt hydrates as latent heat storage materials:Thermophysical properties and costs, Sol. Energy Mater. Sol. Cells 145 (2016) 255–286, http://dx.doi.org/10.1016/j.solmat.2015.10.029.
[84] V. Jülch, Comparison of electricity storage options using levelized cost of storage (LCOS) method, Appl. Energy 183 (2016) 1594–1606, http://dx.doi.org/10.1016/j.apenergy.2016.08.165.
[85] G. Towler, R. Sinnott, Economic evaluation of projects, in: Chemical Engineering Design, Elsevier, 2022, pp. 305–337.
[86] G. Schneider, H. Maier, J. Häcker, S. Siegele, Electricity storage with a solid bed high temperature thermal energy storage system (HTTES) - a methodical approach to improve the pumped thermal grid storage concept, in: Proceedings of the 14th International Renewable Energy Storage Conference 2020, IRES 2020, in: Atlantis Highlights in Engineering, Atlantis PressParis, France, 2021.
[87] O. Schmidt, S. Melchior, A. Hawkes, I. Staffell, Projecting the future levelized cost of electricity storage technologies, Joule 3 (1) (2019) 81–100, http://dx.doi.org/10.1016/j.joule.2018.12.008.
[88] D.O. Kunysz, Kostenschätzung im chemischen Anlagenbau, Springer Fachmedien Wiesbaden, Wiesbaden, 2020, http://dx.doi.org/10.1007/978-3-658-29251-5.
[89] European Central Bank. U.S. dollar (USD), US dollar (USD). URL https://www.ecb.europa.eu/stats/policy_and_exchange_rates/euro_reference_exchange_rates/html/eurofxref-graph-usd.en.html.
[90] J. Koksharov, L. Zendel, F. Dammel, P. Stephan, Thermodynamic, economic and maturity analysis of a carnot battery with a two-zone water thermal energy storage for different working fluids, Energies 17 (2) (2024) 437, http://dx.doi.org/10.3390/en17020437.
[91] A. Seppälä, K. Turunen, M.R. Yazdani, Thermal conductivity of sugar alcohols, Sol. Energy Mater. Sol. Cells 243 (2022) 111796, http://dx.doi.org/10.1016/j.solmat.2022.111796.
[92] V.V. Tyagi, K. Chopra, R.K. Sharma, A.K. Pandey, S.K. Tyagi, M.S. Ahmad, A. Sarı, R. Kothari, A comprehensive review on phase change materials for heat storage applications: Development, characterization, thermal and chemical stability, Sol. Energy Mater. Sol. Cells 234 (2022) 111392, http://dx.doi.org/10.1016/j.solmat.2021.111392.